

# A high resolution opal and radiolarian record from the subpolar North Atlantic during the Mid-Pleistocene Transition (1069–779 ka): Palaeoceanographic implications



I. Hernández-Almeida <sup>a,\*</sup>, K.R. Bjørklund <sup>b</sup>, F.J. Sierro <sup>a</sup>, G.M. Filippelli <sup>c</sup>, I. Cacho <sup>d</sup>, J.A. Flores <sup>a</sup>

<sup>a</sup> Department of Geology, University of Salamanca, 37008 Salamanca, Spain

<sup>b</sup> Natural History Museum of Oslo, University of Oslo, 0562 Oslo, Norway

<sup>c</sup> Department of Earth Sciences, Indiana University-Purdue University Indianapolis (IUPUI), 46202, Indianapolis, USA

<sup>d</sup> GRC Marine Geosciences, Department of Stratigraphy, Paleontology and Marine Geosciences, University of Barcelona, 08028 Barcelona, Spain

## ARTICLE INFO

### Article history:

Received 30 November 2010

Received in revised form 4 May 2011

Accepted 30 May 2011

Available online 28 June 2011

### Keywords:

Radiolarian

Biogenic opal

North Atlantic

Melt-water discharge

Ocean circulation

Productivity

## ABSTRACT

A high-resolution record of radiolarian assemblages from Site U1314 was studied to reconstruct hydrographic and climatic changes in the North Atlantic Ocean during the Mid-Pleistocene Transition period (1069–779 ka). Besides the faunal record, absolute accumulation of radiolarians and total biogenic opal are used to determine changes in surface water productivity. Results show that the North Atlantic Arctic Front shifted back and forth repeatedly at a glacial/interglacial timescale, bringing the site under the influence of both cold Arctic (glacial), and much warmer Atlantic (interglacial) waters. During glacial intervals and “ice-rafted debris” (IRD) events, the deep-dwelling taxon *Cycladophora davisiana* was the greatest contributor of the radiolarian assemblage, suggesting cold surface conditions, melt-water discharge and changes in deep and intermediate circulation. Interglacial intervals were characterized by abundant shallow-dwelling taxa like *Pseudodyctiophimus gracilipes* and *Lithomelissa setosa*, increased opal accumulation, and higher radiolarian diversities, indicating a northward flow of warm Atlantic surface waters to the Site U1314 area. A marked change in the structure of the radiolarian assemblage occurred after MIS 22 (~860 ka), with large taxa differences between warm and cold periods, probably in response to changing ocean conditions due to the higher amplitude of glacial/interglacial changes as the dominant periodicity of high-latitude climate oscillations shifted from 41-kyr to 100-kyr. Thus, we conclude that the radiolarian assemblage from the North Atlantic have changed drastically along with variations in ocean circulation in response to orbital and millennial-scale climatic variations that occurred in the Early and Mid-Pleistocene.

© 2011 Elsevier B.V. All rights reserved.

## 1. Introduction

Sediments in the subpolar North Atlantic Ocean have been the subject of a large number of paleoceanographic studies due to the important role of this region in modulating the global climate (Heinrich, 1988; Bond et al., 1992; Broecker et al., 1992; McManus et al., 1994; Oppo, 1997; McManus et al., 1999). Abrupt changes in the North Atlantic resulted from variations in thermohaline circulation (e.g. Ruddiman et al., 1980; Shackleton et al., 1983) related to extreme cooling of surface waters and enormous amounts of drifting ice (Bond et al., 1992). Besides these cyclical ice-volume fluctuations, Earth's climate system show a gradual trend toward more glacial conditions between 1200 and 500 ka (Head and Gibbard, 2005), the so-called “Mid-Pleistocene Transition” (MPT), related to a shift of global glacial/interglacial cycles from 41-kyr to 100-kyr (Ruddiman et al., 1989; Berger and Jansen, 1994; Raymo and Nisancioglu, 2003; Raymo et al., 2004).

Such environmental changes brought large variations in surface and deep habitats in the ocean, which consequently affected planktonic and benthic communities. Therefore, temporal evolution of fossil assemblages in the sedimentary record provides detailed paleoecological information necessary to reconstruct past climate and hydrographic conditions. Several microfossil groups have been used in paleoceanographic studies in North Atlantic sediments, such as planktonic and benthic foraminifera (Venz et al., 1999; Wright and Flower, 2002; Kawagata et al., 2005), diatoms (Koç and Schrader, 1990; Koç et al., 1993) and coccolithophores (Marino et al., 2008). We focus here alternatively on the polycystine radiolarians, Spummellaria and Nassellaria (hereafter called radiolarians), for reconstruction of the paleoceanographic conditions in the North Atlantic Ocean.

Radiolarians are widely distributed in the world ocean occupying surface and deep habitats with a broad range of physical–chemical water-mass characteristics (e.g. temperature, salinity, nutrients) (Kling and Boltovskoy, 1995; Abelman and Gowing, 1997; Itaki, 2003). Due to this adaptive facility, radiolarians have proven an effective tool in paleoenvironmental reconstructions (Petrushevskaya and Bjørklund, 1974; Morley, 1983; Matul et al., 2002; Cortese et al., 2003). Based on this assumption, we present a new and

\* Corresponding author at: Faculty of Sciences, Plaza de los Caídos s/n. 37008, Salamanca, Spain. Tel.: +34 923 29 44 97; fax: +34 923 29 45 14.

E-mail address: [ihalmeida@usal.es](mailto:ihalmeida@usal.es) (I. Hernández-Almeida).

high-resolution record of radiolarian assemblages and biosiliceous material (opal) accumulation rates from IODP Site U1314 to identify key radiolarian species and their ecological requirements, aimed at reconstructing water-mass structures and productivity regimes during glacial/interglacial cycles in the North Atlantic sediment record. In addition, we investigate the major hydrographic and climatic changes in the North Atlantic during the MPT through variations in radiolarian assemblages.

## 2. Hydrography of the site location

Site U1314 (Fig. 1) is strongly influenced by the northward flow of the North Atlantic Current (NAC). This surface water mass travels northward across the North Atlantic where it crosses the Mid-Atlantic Ridge between 53° N and 60° N. One branch turns northwestwards and travels as the Irminger Current (IC) on the western and northern side of Iceland, mixing with the cold East Greenland Current (EGC), while the main branch flows over the Iceland-Faeroe Ridge into the Greenland, Iceland, and Norwegian (GIN) Seas (Krauss, 1986). This current carries heat to the north and maintains the warm climates of central and northern Europe. Winter convection of the warm and salty Atlantic surface waters in the GIN Seas results in the formation of North Atlantic Deep Water (NADW) that flows as the Iceland-Scotland Overflow Water (ISOW) through the Faeroe Bank channel to enter the Iceland basin (Swift, 1984; Schmitz and McCartney, 1993).

In addition, the flow of the NAC to high-latitudes creates a complex zone of mixing between cold Arctic waters and warm Atlantic waters, named the Arctic Front (AF) (Swift and Aagaard, 1981). During the Pleistocene epoch, subpolar North Atlantic was affected by repeated

changes in climate and water masses at a glacial/interglacial time scale (McIntyre et al., 1999; McManus et al., 1999; Raymo et al., 2004). These variations were a consequence of major north-south migrations of the AF, bringing the site under the influence of both cold Arctic (glacial), and much warmer (interglacial) surface waters.

## 3. Material and methods

### 3.1. Sediment samples and chronostratigraphy

Integrated Ocean Drilling Program (IODP) Site U1314 (2,820 m) was cored by the D/V JOIDES Resolution in the southern Gardar Drift, in the subpolar North Atlantic (56.36°N, 27.88°W) during IODP Expedition 306 (Fig. 1). Site U1314 is located at the northern edge of the glacial North Atlantic Ice Rafted Detritus (IRD) belt (Ruddiman, 1977; Ruddiman and McIntyre, 1981), on the east side of the Reykjanes Ridge, an area of exceptional radiolarian abundance and preservation compared to the relative scarcity in North Atlantic surface sediments (Goll and Björklund, 1971).

The section of Site U1314 studied here comprises 24.16 m with an average sedimentation rate of about 7–7.5 cm/ka for the Pleistocene (Channell et al., 2006). Lithologies consist of nannofossil oozes enriched in biogenic and terrigenous components, and terrigenous silty clay with a varying proportion of calcareous (e.g., nannofossils, foraminifers) and siliceous (e.g., sponge spicules, diatoms and radiolarians) organisms. A more detailed core description is given in Channell et al. (2006).

Conversion from core depth to time was derived by direct correlation of the benthic foraminiferal oxygen isotope record from

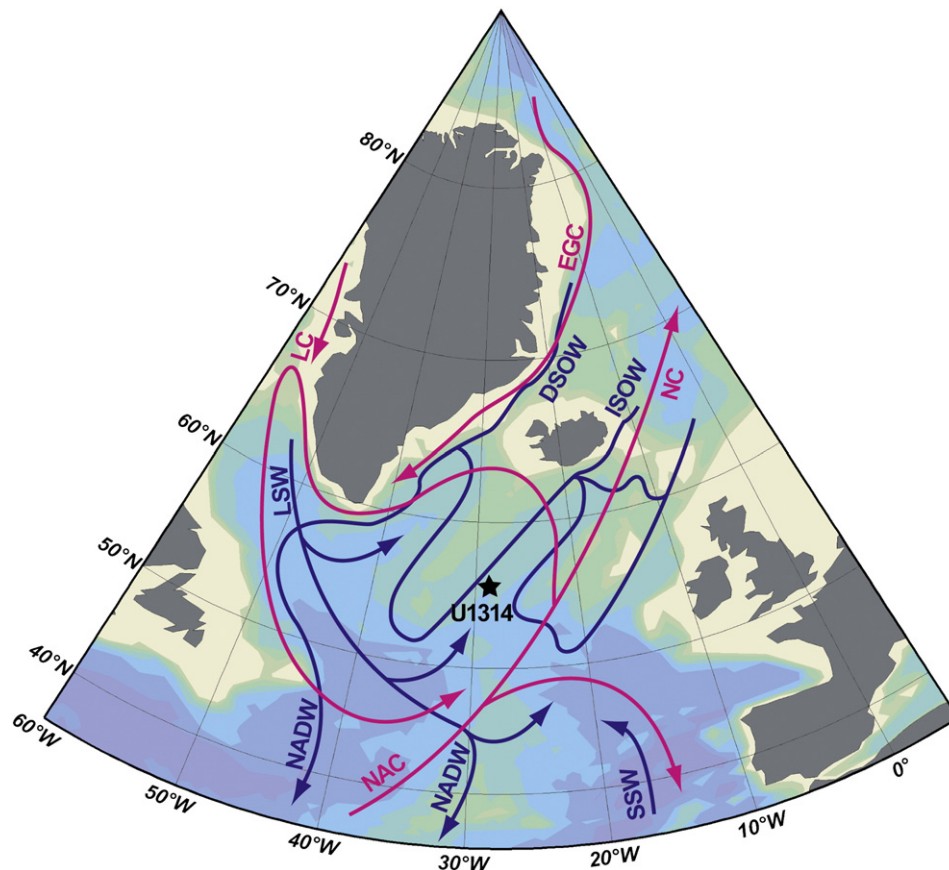


**Fig. 1.** Location of IODP Site U1314 (black star: 56°21'N, 27°W; 2820 m water depth), modern surface (pink), and deep circulation (blue) in the North Atlantic (Krauss, 1986; Schmitz and McCartney, 1993). Map generated with Ocean Data View v.3.4.3. software (Schlitzer, 2008). East Greenland Current (EGC), Norwegian Current (NC), Labrador Current (LC), North Atlantic Current (NAC), Denmark Strait Overflow water (DSOW), Iceland Scotland Overflow water (ISOW), Labrador Sea water (LSW), North Atlantic Deep water (NADW), and Southern Source Waters (SSW).

Site U1314 (Hernández-Almeida et al., in preparation) with the orbitally tuned benthic isotope stack of Lisiecki and Raymo (2005) (hereinafter referred to as LR04) by using *AnalySeries 2.0* software (Paillard and Yiou, 1996). Based on the 13 tie points used to correlate the reference curve LR04 with our benthic oxygen data set, the final age model for the 24.16 m of the core section spans an interval from 1069 to 779 ka, yielding a temporal resolution of 290 kyrs. Between the tie points sedimentation rates were assumed constant, based on the shipboard preliminary stratigraphy (Channell et al., 2006). The orbitally tuned age model and tie points used in it are shown in Fig. 2 and Table 1 respectively.

### 3.2. Methodology

In this micropaleontological study, 299 sub-samples (2 cm thickness taken at 8–16 cm intervals) from Site U1314 were used for the radiolarian analysis. This high sample density yields a time estimate of around 1 kyr between samples. The techniques used to separate the radiolarian skeletons from the sediment follow the Goll and Björklund (1974) procedure. Briefly, samples were oven-dried for 24 h, weighed (1–5 g), and then treated with 15% H<sub>2</sub>O<sub>2</sub> and HCl solutions to remove the organic matter and the calcium carbonate respectively. The samples were then wet sieved (45 µm mesh size), after which two types of slides were made from the residue, one to quantify the radiolarian abundance (Q-slide) and the other for species counts (faunal analysis, F-slide). In addition, a Diatom Index (DI) was determined to evaluate qualitatively diatom and terrigenous material content in our Q-slides, ranging between 1 (sporadic or absent) to 5 (extremely abundant). To prepare the Q-slides, the entire residue from each sample was transferred to a 100-ml beaker that contained 50-ml of distilled water. The solution was then well homogenized, after which a 0.2-ml sample was taken from the suspension using a micropipette and dropped onto a glass slide. The sample was then dried and mounted with Canada balsam. The F-slides were made from

**Table 1**

Tie points used in the correlation between benthic  $\delta^{18}\text{O}$  from Site U1314 and benthic isotope stack LR04.

Site U1314 Depth (mcd)	LR04 Time (ka)
60.10	780.619
61.79	795.244
62.16	807.358
63.12	817.649
68.55	858.636
68.92	872.225
70.99	921.458
71.88	929.571
75.01	951.451
75.50	962.858
77.60	987.871
79.41	1004.220
83.37	1058.727

the remaining residue in the beaker. Radiolarian census counts are based on at least 300 identified specimens at the lowest taxonomic level. During data generation we encountered 79 species (see Appendix A). The taxonomic level of counting was normally at the species level, but ranged from subspecies to undifferentiated family and suborder categories (*Nassellaria* indet. and *Spumellaria* indet., used mainly for juvenile stages that cannot be assigned to species). We have followed the same counting procedure that was used in Björklund et al. (1998) and Cortese et al. (2003), where some selected phaeodarian species were included in the counts. Therefore, the informal name radiolarians include both the selected phaeodarian species and the polycystine taxa shown in Appendix A.

Benthic foraminiferal stable isotope analyses were carried out at the University of Barcelona on a Finnigan MAT 252 mass spectrometer. Due to the scarcity of benthic foraminifera, two species were selected, *Cibicides wuellerstorfi* and *Melonis pompilioides*, to obtain a

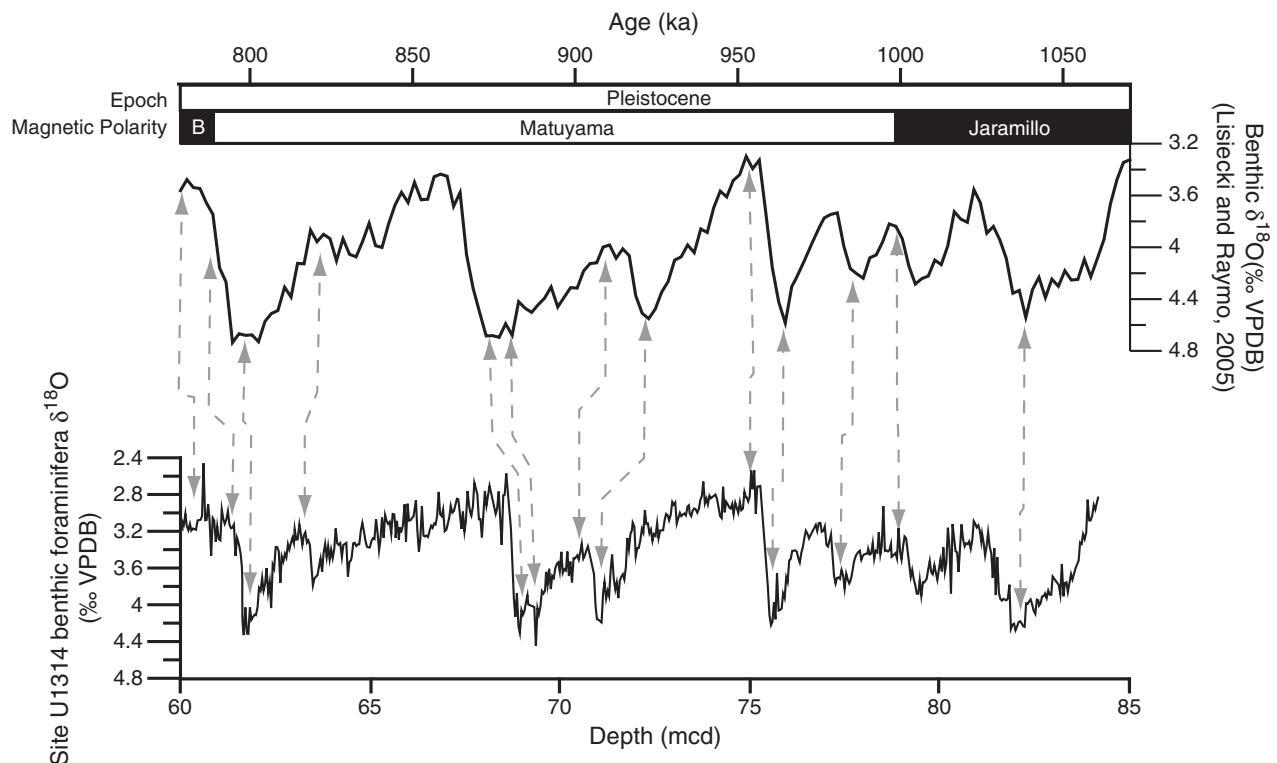


**Fig. 2.** Construction of the age model was performed by correlating the benthic isotope stack of Lisiecki and Raymo (2005) (LR04) with Site U1314 benthic  $\delta^{18}\text{O}$ . Tie points of both records are joined by dashed lines.

continuous record of oxygen and carbon isotopes. Analytical accuracy was better than 0.06‰ for  $\delta^{18}\text{O}$ , and better than 0.02‰ for  $\delta^{13}\text{C}$ . Calibration to the Vienna Pee Dee Belemnite (VPDB) standard scale (Coplen, 1996) was made through the NBS-19 standard.

Biogenic opal accumulation rates (AR) ( $\text{g}\cdot\text{cm}^{-2}\cdot\text{ka}^{-1}$ ) were determined in 572 sub-samples (2 cm thickness taken at 4 cm intervals) following the procedure of Mortlock and Froelich (1989), using 10 ml of 2 M  $\text{Na}_2\text{CO}_3$ , although for this study final opal measuring was determined by using a Leeman Labs P950 inductively coupled plasma-atomic emission spectrometer (ICP-AES) with a CETAC Corp. AT500<sup>+</sup> ultrasonic nebulizer at the Indianapolis University-Purdue University at Indianapolis. The accuracy of our analyses was evaluated by comparison to the long-term results from a consistency standard included in all biogenic opal measurements performed. The average standard deviation was 1.7%.

### 3.3. Taxonomical notes

We have used the taxonomic concept by Hatakeda and Björklund (2009), and illustrations of the species used in the present study are given in Appendix A. Several species have been counted together due to the difficulty of an exact identification with total confidence, particularly of juvenile stages (*Lithomitra lineata* and *Lithomitra arachnea*; *Actinomma boreale* and *Actinomma leptodermum*; *Spongotrochus glacialis* and *Spongodiscus resurgens*). Therefore, these taxa are reported in this study as *L. lineata/arachnea* group, *A. leptodermum/boreale* group and *Spongotrochus glacialis/resurgens* group, respectively.

Additionally, species with a common tropical–subtropical affinity like *Tetrapyle octacantha*, *Pterocanium praetextum*, *Dyctiocoryne profunda*, *Spongocore puella*, *Lithomelissa thoracites*, *Eucyrtidium acuminatum* and *Lamprocyclus maritilis* are good indicators of warm and open ocean conditions in the North Atlantic (Goll and Björklund, 1971; Petrushevskaya and Björklund, 1974; Matul, 1994b; Haslett, 1995). These species appeared during interglacial intervals, but in low percentages too low to be of any importance as individual species. Therefore, and according to Cortese et al. (2003) considerations, we have grouped them as “drift fauna group”.

### 3.4. Statistical analysis

For the diversity/statistical analysis of the radiolarian census data, radiolarian accumulation rate (RAR), and opal AR we used the PAST software (PAleontological STatistics; Hammer et al., 2001). Radiolarian counts converted into percentages were used to calculate the Shannon–Weaver (*H*) diversity index (Shannon and Weaver, 1963). This index, based on a count of species, is sensitive both to changes in the number of species and to changes in the relative abundance of species in a sample. High values can result from an addition of species, greater equality in abundance, or both. A more detailed discussion of this index and its use in ecological studies is provided by (Pielou, 1975).

The multivariate statistics method Detrended Correspondence Analysis (DCA) was applied to our counts, because this is a suitable method for studying gradients in such data sets and to check the response to underlying environmental parameters (Hammer et al., 2001). The species and samples that were used in the DCA had to meet the following criteria, as recommended by Imbrie and Kipp (1971): (1) the species had to occur as more than 1% of the total fauna in at least one sample and (2) had to occur in at least 10 samples. After this selection was applied, 26 species remained for our analysis, of which abundance curves for 18 species are shown (Figs. 4A–I; 5A–I).

Finally, in order to detect a significant underlying temporal pattern in the radiolarian population from Site U1314, we applied multivariate Mantel periodogram spectral analysis to our radiolarian data-set because this method can reveal the underlying mechanism (seasonality, astronomical, or other unknown causes) driving the dynamics of the entire fossil assemblage (Hammer, 2007). For the present study,

following Hammer (2007), we used the same 26 species as for the DCA because they were regularly represented in our samples. A temporal spacing (1089 years) between data points was generated by linear interpolation and an inner product distance measure was chosen for the Mantel correlogram. Moreover, spectral analyses were performed for RAR and opal AR records to determine the dominant frequencies of both signals.

## 4. Results

RAR generally varies inversely with the cyclicity described by the benthic oxygen isotopes from Site U1314. Pearson's *R* correlation coefficient between these two variables is  $-0.403$  (correlation is significant at the 0.01 level), indicating that low RAR values correspond with high benthic  $\delta^{18}\text{O}$ . The total radiolarian abundance ranged from barren to 30,000 tests/g at Site U1314 (Fig. 3C, red filled). Periods of high RAR in Pleistocene sediments from the North Atlantic coincide with interglacial conditions, except during MIS 23 (Fig. 3C). On the other hand, glacial periods are poor in RAR and sometimes opal-barren, as also reported by Ciesielski and Björklund (1995). The number of taxa varies between a maximum of 52 species at MIS 21, and a minimum of 7 species at MIS 22. Comparison of the RAR with opal AR at site U1314 shows that many of the opal maxima (Fig. 3C, dashed red line) coincide with high levels of RAR (Fig. 3C), and with diatom abundance, as indicated by the DI (Fig. 3D).

Radiolarian skeletons were well-preserved in all examined samples without any sign of significant dissolution or breakage. There are no large peaks of opal AR with low radiolarian concentrations (Fig. 3C) or low DI (Fig. 3D), which suggests a good generalized preservation of the biogenic fossils also in the  $<45\ \mu\text{m}$  size fraction. Another proxy indicative of opal preservation is the phaeodarian abundance (Stadum and Ling, 1969; Casey et al., 1979), since their skeletons are more unstable as they contain less biogenic silica, having a porous or spongy structure, and are therefore more easily dissolved than the polycystine radiolarians (Takahashi et al., 1983). In our samples, the presence of the phaeodarian taxa *Euphysetta nathorstii* and *Lirella mello* were more frequent during periods with moderate  $\delta^{18}\text{O}$  values, such as during MIS 21, 25 and 27 (Fig. 3C, blue dots), indicating better conditions for opal preservation during interglacial intervals with moderate to high RAR and opal AR.

Of the total of 79 identified taxa of polycystine radiolarians, only the 26 species that accounted for more than 1% on average have been used in the discussion. Comparing the relative abundance curves of these dominant species, we found that most of them had a distribution pattern closely similar to total radiolarian abundance, except for *C. davisiana*. According to our faunal results, and in agreement with previous studies of the North Atlantic radiolarian fauna (Matul, 1989a,b, 1994a, 1994b; Matul and Yushina, 1999), *Cycladophora davisiana* dominates the assemblage during glacial periods (Fig. 4A), while *Pseudodyctiophimus gracilipes* dominates during interglacial periods (Fig. 4F).

Comparison of the distribution pattern of *C. davisiana* (Fig. 3E) with the oxygen isotopic record of Site U1314 (Fig. 3A) revealed that most peaks of this species occurred during glacial stages or at glacial–interglacial transitions. High abundances, however, were also observed during weak interglacial stages (MIS 23) as well as in significant cool periods within prominent interglacial stages (MIS 21). Our sample spacing also shows the rapid change in abundance of *C. davisiana* at the glacial/interglacial transitions, switching from percentages close to 80% to 20% in less than 3 kyr (MIS 22/21, 24/23, 26/25). Additionally, high percentages of *C. davisiana* appear closely related to spikes in the IRD AR (Fig. 3E) and when benthic  $\delta^{18}\text{O}$  values exceed 3.5‰ (Fig. 3A). The *Lithomitra lineata/arachnea* group (Fig. 4B) shows prominent peaks preceding or together with those of *C. davisiana* (e.g. 1056, 981, 965, 868). Likewise, *Larcopyle weddellium* and *Spongopyle osculosa* (Fig. 4D and C respectively) appear to be related to the *C. davisiana* distribution

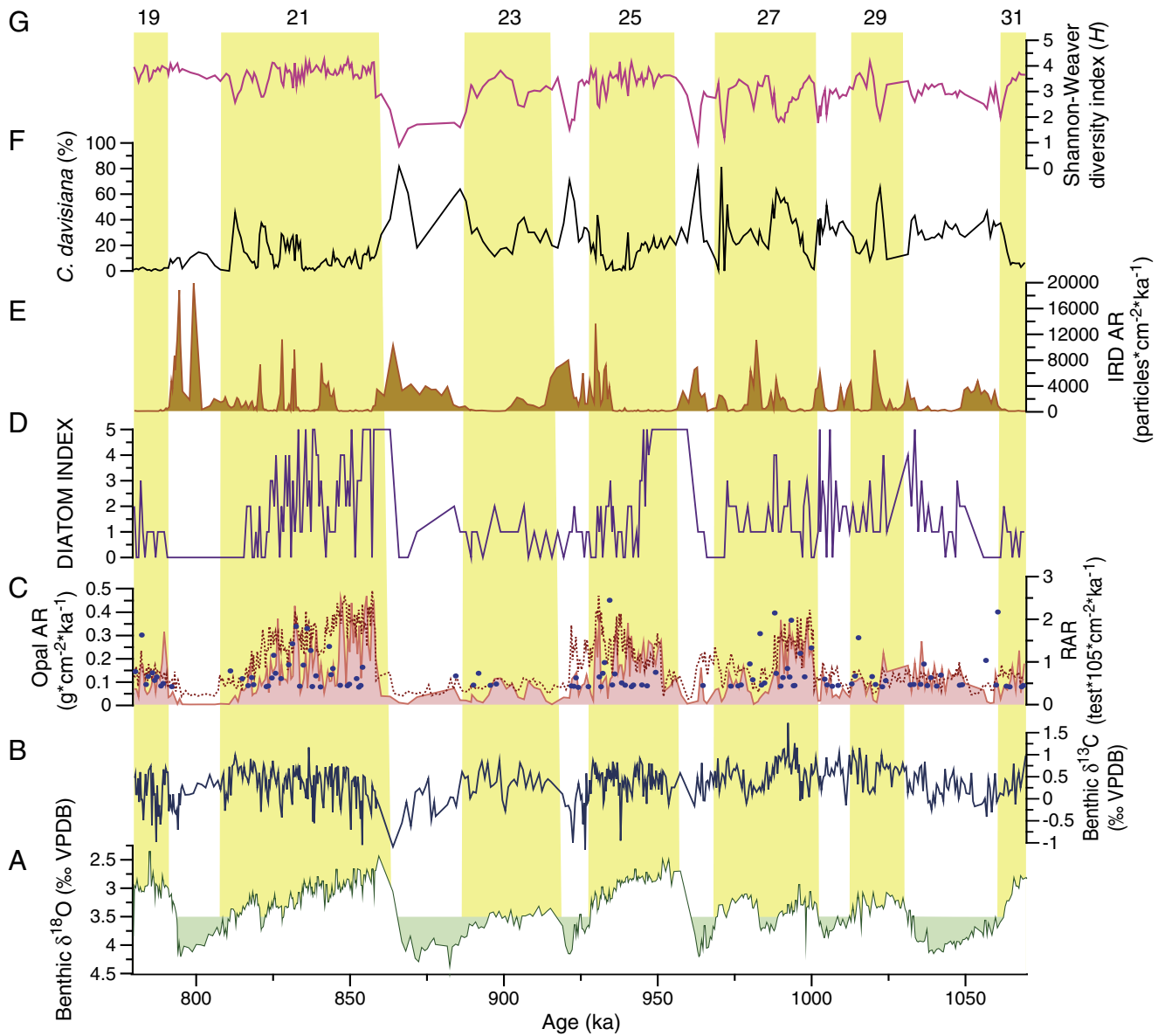


**Fig. 3.** Site U1314 records from 779 to 1069 ka. From bottom to top: a) benthic  $\delta^{18}\text{O}$ , with green filled up to 3.5‰, the glacial threshold (McManus et al. 1999); b) benthic  $\delta^{13}\text{C}$ ; c) RAR (red filled), opal AR (dashed red line) and phaeodarian main percentage peaks (blue dots); d) Diatom Index; e) IRD AR; f) percentage of *C. davisiana* and g) Shannon–Weaver diversity index. Marine Isotope Stages (MIS) are shown at the top.

(Fig. 4A), since they peak at IRD events (e.g. at 821, 868 and 1005 ka). Other abundant species, *Actinomma leptodermum/boreale* group, *Pseudodictyophimus gracilipes*, *Lithomelissa setosa*, *Phorthicum clevei*, “drift fauna group”, *Actinomma medianum*, *Spongotrochus glacialis/resurgens* group, *Stylochlamyidium venustum*, *Larcoyle buetchslii*, *Larospira minor*, *Botryostrobus auritus/australis* group, *Stylodictya validispina*, *Druppratractus variabilis*, *Lithocampe platycephala* (Figs. 4E–I; 5A–D), appeared mainly along interglacial intervals, although some of them showed rather diverse distribution patterns. *A. leptodermum/boreale* group showed increased abundances during MIS 22, 26, during the transitions 20/19, 22/21, 26/25, and at sub-stages of MIS 21 (Fig. 4E). *L. platycephala* spikes occurred mainly during interglacial periods (Fig. 5H), although maxima (5–6%) are displaced toward the end of the interglacial or at benthic  $\delta^{18}\text{O}$  values between 3.5 and 3‰ (Fig. 3A).

Phaeodarians (*Lirella mello* and *Euphysetta* spp.) are little represented in our samples, and they occur normally during periods of

moderate to high RAR within interglacial periods (Fig. 3C blue dots). The Shannon–Weaver diversity-index ( $H$ ) shows a distribution pattern following glacial/interglacial units (Fig. 3G) and is negatively correlated with the distribution of the deep-living taxon *C. davisiana*. Higher  $H$  values were recorded during light  $\delta^{18}\text{O}$  values (interglacial stages) and low percentages of *C. davisiana*, and vice versa (Fig. 3F–G).

The results of the DCA of the radiolarian data from Site U1314 are shown in Fig. 7. Axes eigenvalues (A1: 0.20; A2: 0.08; A3: 0.06) indicate the amount of variation in the dataset explained by each axis. In our DCA only Axis 1, which explain about 23% of the total variation, is discussed, since Axes 2 and 3 have very low variance (<0.1%) and explain only 17% of the variation (9% and 8.1%, respectively), and therefore are of uncertain interpretation (Hammer, personal communication). Samples with higher positive Axis 1 values correspond to cold isotope stages 26 and 22. Likewise, the species *C. davisiana*, *S. osculosa* and *L. lineata/arachnea* group that nowadays have optimum abundances in sediments below cool waters and glacial environments

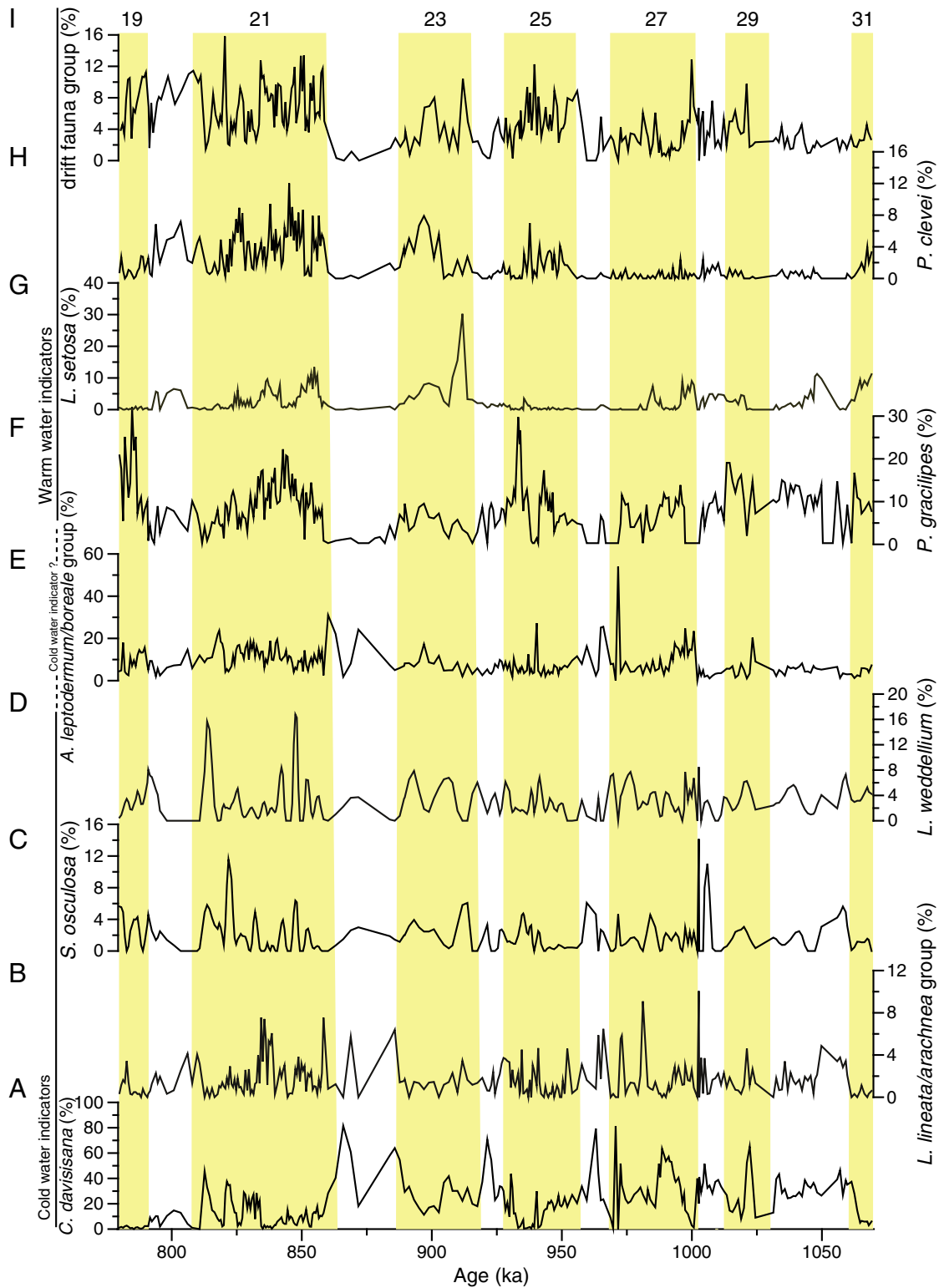


Fig. 4. Radiolarian species representing more than 1%. Water mass affinity according to DCA represented in vertical left-side line and text.

(e.g. Petrushevskaya and Björklund, 1974; Björklund et al., 1998; Okazaki et al., 2004; Abelmann and Nimmergut, 2005), are also placed at the positive side of the Axis 1. Furthermore, typical warm-condition species like *P. clevei* and *A. medianum* (Björklund et al., 1998; Lüer, 2003) are located on the opposite side (negative values) of the Axis 1. Species that tolerate a wide range of temperature variance and also prefer

mixing environments, like *P. gracilipes* (Björklund et al., 1998), are placed in the middle of the gradient (Fig. 7). Based on this distribution pattern of species and samples in the DCA (Fig. 7), we have inferred that a combination of factors associated with changing conditions in the water column between glacial and interglacial periods (e.g. IRD input, ice-volume, nutrients, sea-surface temperature and salinity) is the

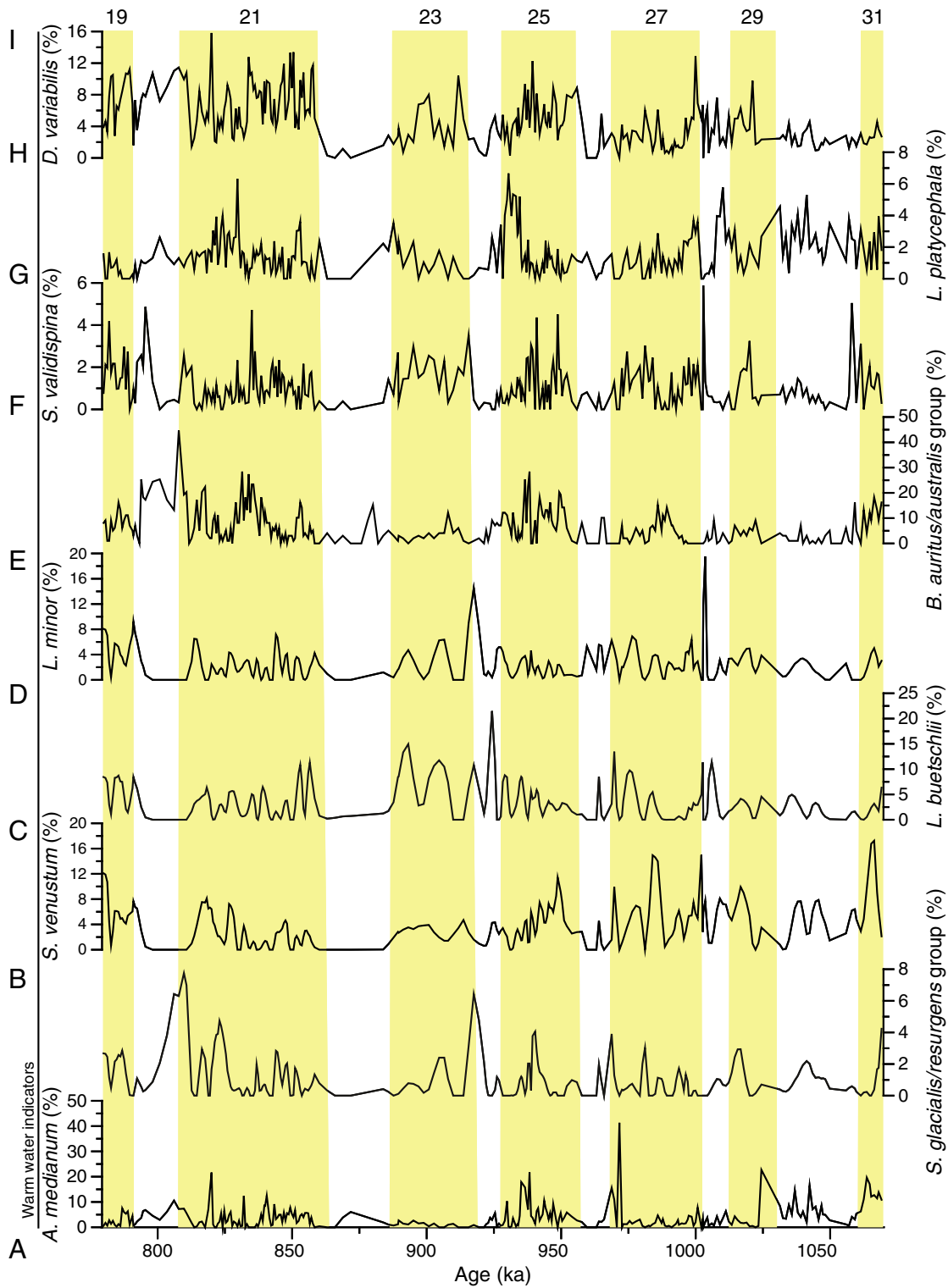


Fig. 5. Radiolarian species representing more than 1%. Water mass affinity according to DCA represented in vertical left-side line and text.

underlying variable related to Axis 1, thus being responsible for gradation within the radiolarian assemblages from Site U1314.

Mantel correlogram and spectral analysis (Lomb periodogram) of the radiolarian assemblage, RAR, and opal AR records respectively, are shown in Fig. 8. Main periodicities are centered in Milankovitch orbital parameters of obliquity (~41 kyr), precession (~23 kyr), and to a lesser extent eccentricity (~100 kyr).

### 5. Discussion

Using the temporal distribution of the most frequent radiolarian taxa (>1%) at Site U1314 and the results obtained from the DCA, we have reconstructed water paleoceanographic and climatic conditions in the North Atlantic Ocean along glacial and interglacial stages. Additionally, for our ecological interpretation and radiolarian species

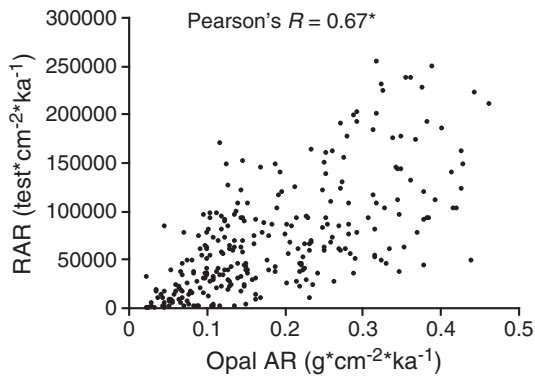


Fig. 6. Correlation between RAR and opal AR. \* Correlation is significant at  $p < 0.01$  level.

water mass affinity, we have used published data concerning the radiolarian distribution in the surface sediments of the North Atlantic and the GIN-Seas (Goll and Björklund, 1971; Petrushevskaya and Björklund, 1974; Matul, 1989a, 1994a, 1994b; Björklund et al., 1998; Matul and Yushina, 1999; Cortese et al., 2003).

### 5.1. The glacial ocean

Glacial ocean in the subpolar North Atlantic is characterized by south-eastward shifts of the AF and expansion of cold Arctic waters to meridional latitudes. These swings are accompanied by seasonal formation of sea-ice, and a more restricted distribution of the warm surface waters, NAC, in the North Atlantic, limited to a narrow flow compressed to the Norwegian continental margin (Van Nieuwenhove et al., 2008). Surface and deep conditions become more dramatic during episodes of large influx of terrigenous material to the ocean triggered by periodic surges of icebergs from North Atlantic

continental margins (Bond et al., 1992; Alley and MacAyeal, 1994; Hemming, 2004; Moros et al., 2004). Enhanced melt-water flux associated with these surges caused a great impact in thermohaline circulation by reducing convective overturning and weakening the deep convection in the GIN Seas (Maslin et al., 1995; Vidal et al., 1997).

This hydrographic scenario caused a large drop in surface primary productivity, as seen in the low DI values at Site U1314 and strong reduction in diatom abundance at neighbor site 983 during MIS 26, 24 and 22 (Koç et al., 1999), and led to a drastic reduction in the radiolarian fauna. Most of radiolarian species observed at Site U1314 do not tolerate low SST that accompanied ice-sheet advances, and consequently migrated to southern latitudes. Taking into account these considerations, we suggest increasing percentages of *C. davisiana* during glacial stages and IRD discharges must be related to the reduced number of other species and development of unique conditions in the North Atlantic during these periods.

Nowhere in present day oceans *C. davisiana* abundances account for more than 5% of the total assemblage (Morley and Hays, 1979, 1983; Morley, 1983; Matul, 1989b; Björklund and Ciesielski, 1994), except for the Okhotsk Sea, where *C. davisiana* exceeds 30% (Nimmergut and Abelmann, 2002; Hays and Morley, 2003; Okazaki et al., 2003, 2004; Abelmann and Nimmergut, 2005; Itaki et al., 2008). The favorable conditions for *C. davisiana* in the Okhotsk Sea are closely related to well-ventilated, low-temperature, and oxygen-rich intermediate waters (Nimmergut and Abelmann, 2002; Itaki, 2003; Abelmann and Nimmergut, 2005) and the supply of organic matter (Nimmergut and Abelmann, 2002; Hays and Morley, 2003; Okazaki et al., 2003; Abelmann and Nimmergut, 2005). This hydrographic context occurs during periods of low surface salinities combined with extensive sea-ice (Rogachev, 2000). Hence, based on these observations, we speculate that high *C. davisiana* abundances at Site U1314 reflect prolonged periods of sea-ice cover, increased levels of sea-ice and/or iceberg melt water producing low salinity surface waters, and

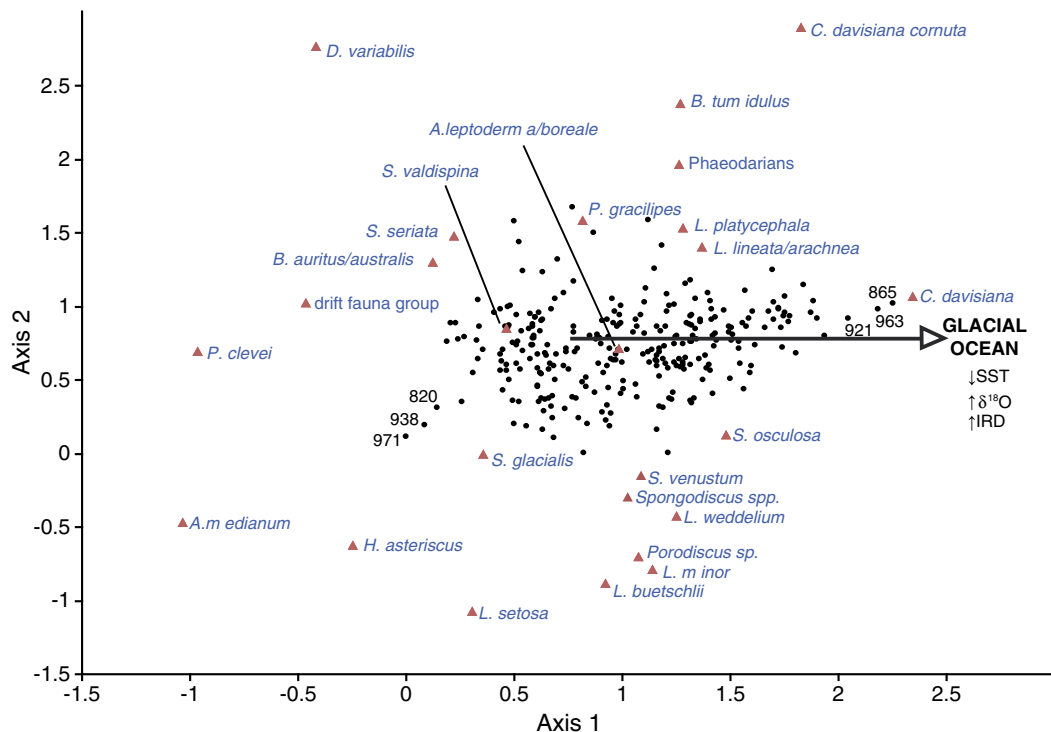
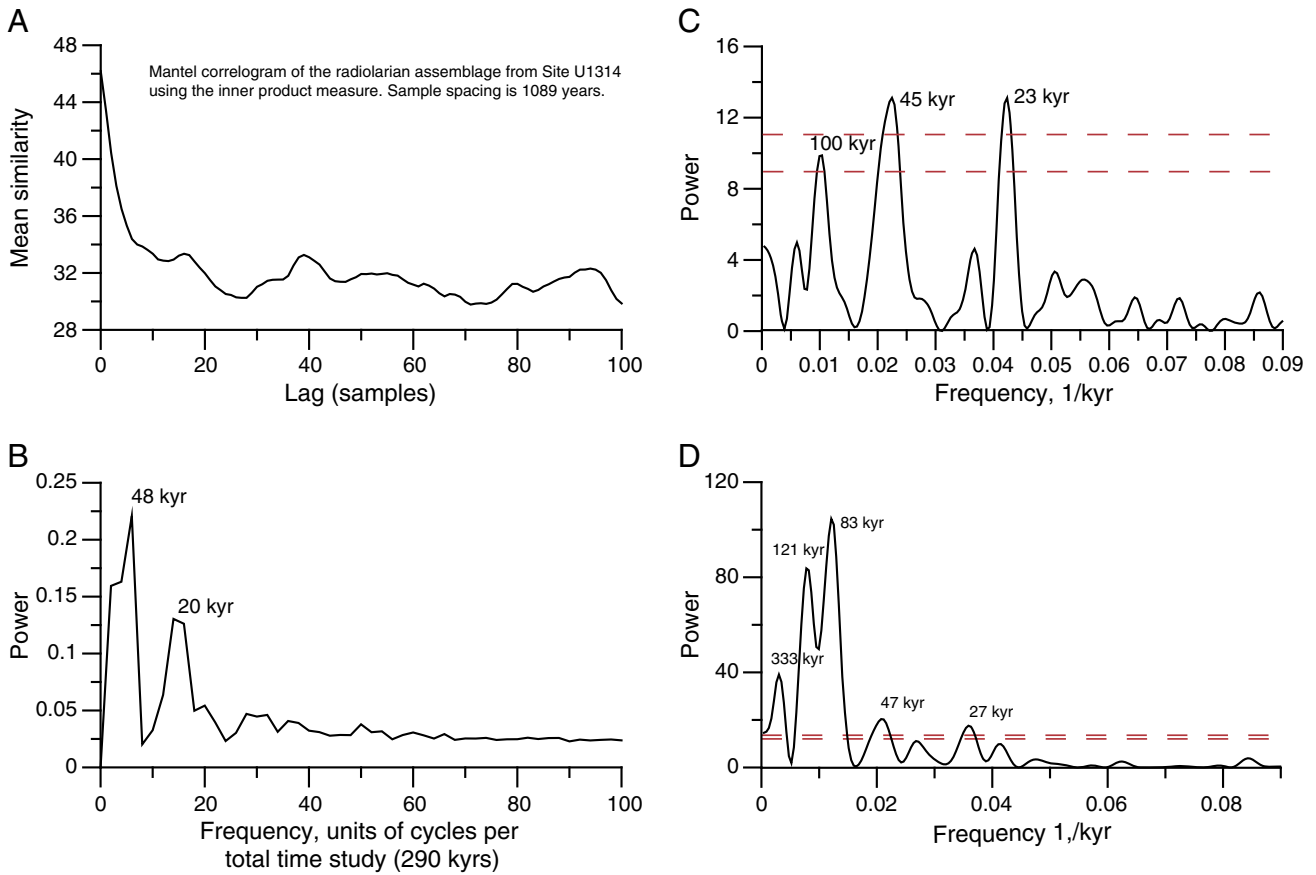


Fig. 7. DCA diagram of the radiolarian species (red triangles) and samples (black dots) from Site U1314. Only samples occupying extreme positions along Axis 1 have been labeled with the age (ka). Arrows indicate inferred (environmental) variables.



**Fig. 8.** A) Mantel correlogram of the multispecies time series for the interval 779–1069 ka using inner product measure (sample spacing is 1089 year) and B) time spectra using the discrete Fourier transform of the Mantel correlogram. See Hammer (2007) for procedure description. Spectral analysis (Lomb periodogram) of the different paleoceanographic records from Site U1314: C) RAR and D) opal AR for the same interval. Numbers above peaks denote respective periodicities. The 0.01 and 0.05 significance levels ('white noise lines') are shown as red dashed lines.

the establishment of a shallow temperature minimum, with relatively stable temperatures and salinities at depths below this minimum. During glacial times, convection in the GIN Seas switched from a deep to intermediate mode (Oppo and Lehman, 1993, 1995). Therefore, intensification of a cold oxygenized intermediate water mass, accompanied by low surface temperatures and salinities due to melt-water input during iceberg discharges, would result in a reduction of radiolarians living in surface water and a dominance of *C. davisiana* in the North Atlantic, as it is observed in the Okhotsk Sea (Nimmergut and Abelmann, 2002; Abelmann and Nimmergut, 2005). This interpretation is further supported by the shifts toward negative values in the benthic foraminiferal  $\delta^{13}\text{C}$  from Site U1314 (2820 m depth) during *C. davisiana* peaks (Fig. 3B, F), indicating a reduction in deep water production at depths lower than 2000 m and enhanced ventilation at shallower depths (Venz et al., 1999; Flower et al., 2000; Kleiven et al., 2003). At these times, deep water in the North Atlantic may have formed by brine rejection under sea ice on the continental shelves by processes more analogous to those observed around Antarctica today (Vidal et al., 1998; Dokken and Jansen, 1999; Raymo et al., 2004). Hence, as suggested by Itaki et al. (2009), organic matter that serves as a food source for *C. davisiana* would be released into the intermediate-water depths via a brine pumping process during winter sea-ice formation.

Hydrographic conditions inferred for high percentages of *C. davisiana* at Site U1314 are corroborated by the concomitant increases of the polar foraminifera *Neogloboquadrina pachyderma sinistrorsa* (sin.) at Sites 980 and 984, for the time interval over which

these two records overlap (1000–779 ka) (Wright and Flower, 2002). In North Atlantic marine sediments, rapid increases in the abundance of *N. pachyderma* sin. correspond to a major reduction in planktonic foraminifer abundance, linked with changes in primary productivity, and changes in temperature and/or salinity related to AF fluctuations and massive iceberg discharges (Bond et al., 1992; Johannessen et al., 1994; Bond and Lotti, 1995; Pflaumann et al., 2003). Hence, we suggest that high percentages of *C. davisiana* significance in Early and Mid-Pleistocene sediments at Site U1314 would be analog to that of the polar planktonic foraminifera *N. pachyderma* sin. in the North Atlantic.

It has been proposed to consider the Quaternary variations in *C. davisiana* abundance as analogous to the oxygen isotope curves in the cold-water areas of the ocean (Morley and Hays, 1979, 1983; Hays and Morley, 2003). A detailed examination of the relationship between glacial–interglacial conditions and *C. davisiana* peaks, reveals that high abundances of the species occurred when benthic  $\delta^{18}\text{O}$  values were around 3.5‰ and the highest abundances coincide with  $\delta^{18}\text{O}$  more than 4‰ (Fig. 3A, F), as previously noted by Ciesielski and Björklund (1995). This observation is supported by correlation between Axis 1 samples scores and benthic  $\delta^{18}\text{O}$  values (Table 2); the higher oxygen isotope values, radiolarian assemblage is more dominated by species located at right side of Axis 1, like *C. davisiana*. The boundary of 3.5‰ in benthic  $\delta^{18}\text{O}$  for increased *C. davisiana* populations is the same threshold as proposed by McManus et al. (1999) as the minimum ice-volume required to trigger large instabilities in the North Atlantic ice-sheets. This close relationship

**Table 2**

Correlation matrix between Axis 1 from DCA and Site U1314 proxies. The bold values correspond to significant correlations at  $p < 0.01$  level.

	RAR	Benthic $\delta^{18}\text{O}$	IRD AR
Axis 1	<b>-0.223</b>	<b>0.458</b>	<b>0.348</b>

between *C. davisiana* and high benthic  $\delta^{18}\text{O}$  values also showed up in the position of *C. davisiana* along the Axis 1 of the DCA (Fig. 7), next to the samples with heaviest oxygen isotopic values. Hence, rapid variations in *C. davisiana* abundance corresponding to drastic turnovers (Terminations, IRD events and initial phases of glaciations), related to the benthic  $\delta^{18}\text{O}$  threshold of 3.5‰, that would indicate changes in the formation of intermediate and deep water masses accompanying climate fluctuations.

Ubiquity of *C. davisiana* in glacial Early and Mid-Pleistocene sediments is a common feature in the North Atlantic, since high percentages of this species have been also observed in other neighbor sites 114, 609 and 646 (Benson, 1972; Ciesielski and Björklund, 1995). In this sense, it is striking that lower than expected *C. davisiana* percentages during MIS 20 at Site U1314 and former sites (Fig. 3F), were also observed in the Okhotsk Sea (Matul et al., 2009). Since *C. davisiana* relative abundance patterns appear to be synchronized worldwide (Morley and Hays, 1979; Morley et al., 1982), this similarity between North Pacific and the North Atlantic oceans may represent an environmental change at global scale.

*Larcopyle weddellium* and *Spongopyle osculosa* have been listed as intermediate-deep species in several regions (McMillen and Casey, 1978; Casey et al., 1979; Kling and Boltovskoy, 1995; Abelman and Gowing, 1997). At Site U1314, both taxa appear frequently associated with the high *C. davisiana* percentages that also characterize the IRD events. Molina-Cruz (1977a) observed high percentages of *Spongurus* sp. (= *L. weddellium*) associated with *C. davisiana* in coastal and cool waters of the southeast Pacific during episodes of low radiolarian productivity due to very high rates of terrigenous supply. In the same sense, Dow (1978) reported that *S. osculosa* is also highly correlated with high percentages of *C. davisiana* and IRD in the Pleistocene sediments of the Indian Ocean. Okazaki et al. (2004) related *S. osculosa* to unfavorable conditions in the surface waters of the Okhotsk Sea due to seasonal formation of sea-ice (low sea surface salinities and temperatures). Environments described by previous authors therefore suggest conditions very similar to those when IRD was discharged at Site U1314, meaning a water column more suitable for the development of deep-dwellers, due to fresher surface water, causing stratification of the upper water layer.

On the other hand, the *Lithomitra lineata/arachnea* group (Fig. 4B) shows discrete percentages along the studied period, although several significant peaks (3–9%) appear close to the IRD peak together with high *C. davisiana* abundances (e.g. at 1056, 981, 965, 868). Hass et al. (2001) and Molina-Cruz (1991) also reported *L. lineata* together with *C. davisiana* and continental terrigenous supply, and depicted this assemblage as an indicator of a clear Arctic environment, influenced mainly by sea-ice conditions and related to southward migrations of

the AF in a short time-scale. Petrushevskaya and Björklund (1974) concluded that the cosmopolitan species *L. lineata* preferentially inhabits deep waters in cold water regions, together with *Artostrobos annulatus* and *C. davisiana*, as observed in our samples. Moreover, Petrushevskaya (1971a) included *L. arachnea* in her list of species with positive preservation potential, so its increase during IRD and glacial periods may be due to its high resistance to dissolution. Therefore, the *L. lineata/arachnea* group peaks in our samples may indicate cooling conditions during the progressive southward expansion of the AF.

Following *C. davisiana* peaks, at cold and deglacial events, once the adverse conditions for the development of shallow species ended (extensive sea-ice conditions) *Actinomma boreale* and *A. leptodermum* bloomed (Swanberg and Eide, 1992). Numerous authors have reported high abundances of the *A. leptodermum/boreale* group (Petrushevskaya and Björklund, 1974; Swanberg and Eide, 1992; Molina-Cruz and Bernal-Ramirez, 1996; Björklund et al., 1998; Hass et al., 2001) in the Greenland and Iceland Seas related to Arctic or cold Atlantic surface waters, and hence, they seem to be adapted to cold-water conditions. Therefore, increased abundances of the *A. leptodermum/boreale* group during cool and transitional periods suggest Arctic or cold Atlantic environments with open oceanic conditions.

## 5.2. The interglacial ocean

Since total biogenic opal and the radiolarian content are generally used to infer ocean productivity, variability in the radiolarian assemblage can also be a good proxy to for monitoring changes in surface water processes. *P. gracilipes* and *L. setosa* are small-sized nassellaria strongly linked to warm water masses in the Norwegian Sea (Cortese et al., 2003) under conditions of high primary productivity and eutrophic conditions (Yamashita et al., 2002). *P. gracilipes* (Fig. 4F) and *L. setosa* (Fig. 4G) show a distribution pattern that is parallel to those of RAR and DI (Fig. 3C–D). Accordingly, both species are directly related with increased primary productivity associated with increased influence of the warm NAC and water column water mixing (Swanberg and Eide, 1992; Takahashi, 1997)

In the same sense, occurrence of shallow water (upper 200 m) and temperate conditions species *P. clevei* (= *P. pylonium*), *S. glacialis/resurgens* group, *L. buetchslii*, *S. venustum*, *S. glacialis/resurgens* group, *L. minor*, *Botryostrobus auritus/australis* group, *A. medianum*, *Stylodictya validispina* (McMillen and Casey, 1978; Samtleben et al., 1995; Boltovskoy et al., 1996; Hass et al., 2001; Matul et al., 2002; Hays and Morley, 2003; Lüer, 2003; Okazaki et al., 2004; Abelman and Nimmergut, 2005) during interglacial periods (MIS 31, 29, 27, 25, 21) would indicate a northward position of the AF and stronger transport of the NAC, which brings warm waters to high latitudes and originates the high productivity conditions in the area of Site U1314 (Goll and Björklund, 1971; Matul, 1989b, 1994a; Björklund et al., 1998; Matul and Yushina, 1999; Hatakeda and Björklund, 2009). A similar response is shown by *Druppatractus variabilis* (= *Druppatractus cf. pyriformis*) (Fig. 5I), considered a surface-dweller of warm-waters in the Gulf of California, where it reaches high abundances with development of oceanic fronts (Molina-Cruz, 1988; Molina-Cruz et al., 1999).

*S. venustum* (Fig. 5C) and *S. glacialis/resurgens* group (Fig. 5B), both indicative of open ocean conditions (Okazaki et al., 2003), show some

## Plate I.

- 1–4. *Actinomma boreale* Cleve, 1899. 1. Hole C; core 7; section 5; cm 146–148 (64.46 mcd). 2–3. Hole B; core 9; section 2; cm 124–126 (77.84 mcd). 4. Hole C; core 8; section 6; cm 30–32 (75.20 mcd).
- 5–8. *Actinomma leptodermum leptodermum* (Jørgensen, 1900). Hole C; core 7; section 5; cm 146–148 (64.46 mcd).
- 9–11. *Actinomma medianum* Nigrini, 1967. 9–10. Hole C; core 8; section 4; cm 98–100 (72.88 mcd). 11. Hole C; core 8; section 5; cm 2–4 (73.42 mcd).
12. *Actinomma popofskii* (Petrushevskaya, 1967). Hole C; core 8; section 6; cm 30–32 (75.20 mcd).
13. *Actinomma trinacrium* Haeckel, 1862. Hole C; core 7; section 5; cm 146–148 (64.46 mcd).

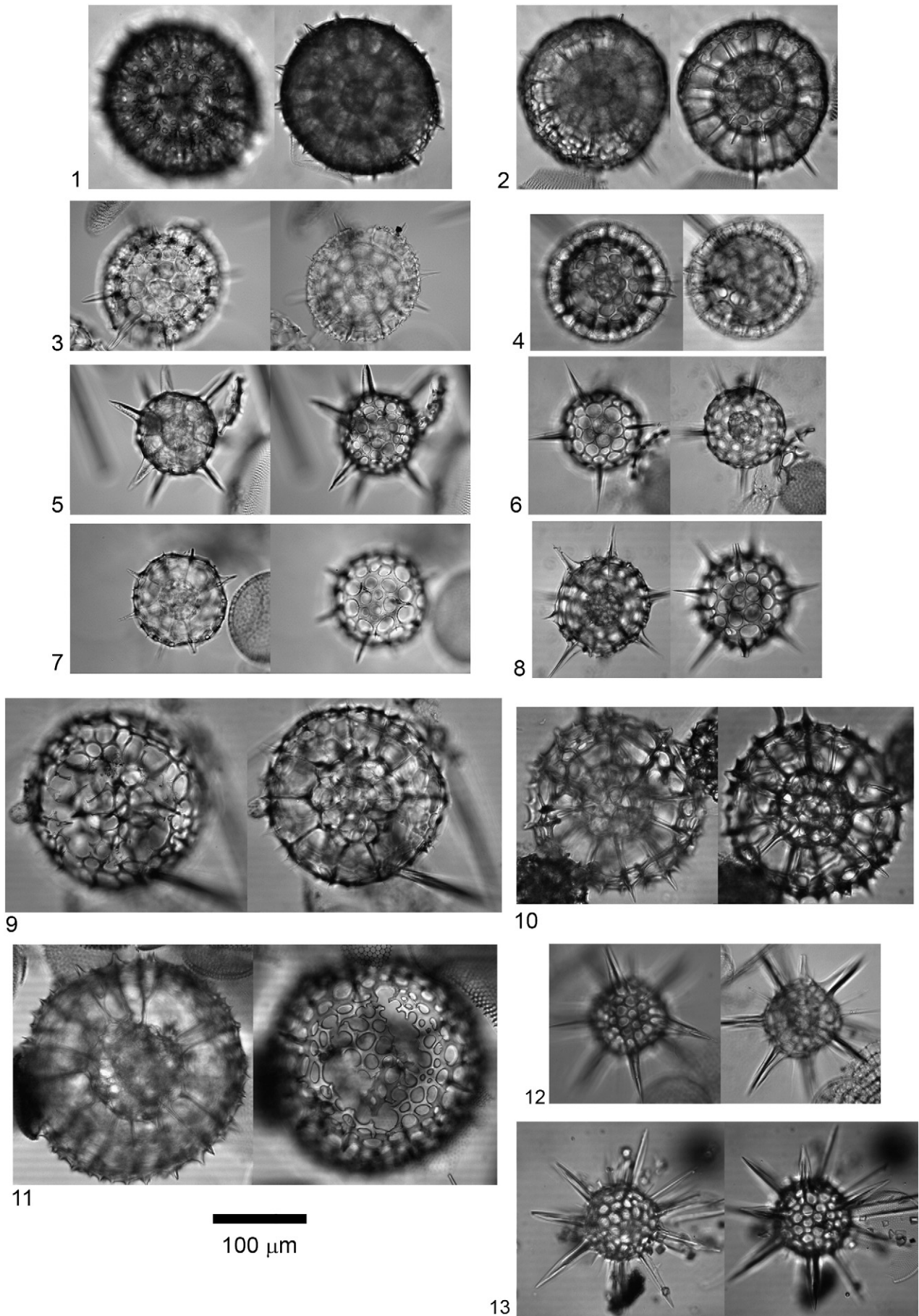


Plate I.

peaks during low RAR (e.g. at 917 and 904 ka). This can be explained by the high adaptability to adverse surface conditions, like low temperature and salinity with strong seasonal changes (Nimmergut and Abelmann, 2002). Moreover, *S. glacialis/resurgens* group, *S. venustum*, and other radiolarians belonging to Spongodiscidae family (*Spongodiscus* sp., *Porodiscus* sp. and *S. validispina*) are particularly resistant (Takahashi and Honjo, 1983; Boltovskoy et al., 1993), allowing easier identification of incomplete shells, thus increasing considerably their abundances in our samples.

*L. platycephala* occurs during cool periods, according to the benthic  $\delta^{18}\text{O}$  values. This species inhabits subarctic waters in the modern Iceland and Greenland seas, in the mixing area of Arctic and Atlantic waters (Molina-Cruz and Bernal-Ramirez, 1996; Björklund et al., 1998; Cortese et al., 2003). Consequently, *L. platycephala* in our samples is related to the southward migration of Arctic waters during the beginning of glaciations.

As discussed previously, *C. davisiana* generally accounts for less than 5% in the modern North Atlantic and in surface sediments (Petrushevskaya and Björklund, 1974; Björklund et al., 1998); we can therefore assume that samples with the lowest percentages of *C. davisiana* at Site U1314 correspond with fully developed interglacial conditions similar to present day ocean, with a resumed deep convection in the Nordic Seas that ventilates the North Atlantic at all depths (Venz et al., 1999). In contrast, *C. davisiana* abundances exceeding 20% in some samples located within interglacial stages may correspond to significant cool periods within robust interglacial stages (at 821 and 827) or weak interglacial stages (at 906, 970, 988 and 1022). This is further confirmed by the absence of *L. setosa* (<1%) and high percentages of *S. venustum* (up to 11%), which tolerates a wide range of temperatures and salinities (Nimmergut and Abelmann, 2002; Abelmann and Nimmergut, 2005), as during early MIS 25. This suggests that some input of cold and low salinity waters reached the area of Site U1314 during this interglacial stage and increased the percentages of *S. venustum* and *C. davisiana*, causing a decrease in *L. setosa* abundance.

Finally, we interpret increased values of “drift fauna group” during interglacial as enhanced NAC episodes that transport them to the subpolar North Atlantic. These species are intruders from tropical waters and can probably not live and reproduce at latitudes as high as 58° N (Björklund and Kruglikova, 2003; Cortese et al., 2003). Consequently, they drifted passively up to the Site U1314 location and do not represent “in-situ” radiolarian production.

### 5.3. Changes in radiolarian and opal accumulation at Site U1314

Global ocean distribution of radiolarians, as in other important opaline plankton groups (diatoms and silicoflagellates), is dependent

on several major environmental parameters, although several authors have highlighted the close affinity of this group to food availability among other factors (Petrushevskaya and Björklund, 1974; De Wever et al., 1994; Boltovskoy et al., 1996). Determination of RAR, in combination with opal AR, may serve as a first-order approximation of past levels of surface productivity, but with some limitations because of possible differential dissolution problems at the sediment water interface (Broecker and Peng, 1982; Takahashi, 1994). Nevertheless, decrease in bulk sediment porosity during IRD deposition would reduce water content, and hence would limit exchange with silica unsaturated bottom waters and better preserve opal microfossils (Nave et al., 2007). In addition, penetrations of silica-rich southern source waters far into the high northern latitudes during decreased relative glacial production of NADW (Marchitto et al., 2002) would help for major opal preservation in North Atlantic sediments. Consequently, we discard opal dissolution as a mechanism for the lower RAR observed at IRD events.

Opal generally accumulates in sediments when diatom and radiolarian production is high, and therefore the primary signal related to opal production is quite relevant in view of the paleoceanographic utilization of opal accumulation data, where emphasis is placed on production rather than on preservation processes (Cortese et al., 2004). Our opal AR, conforms well to the general pattern of the RAR and the DI at Site 1314 (Fig. 3C–D), suggesting that both signals reflect large-scale changes in the amount of microfossil silicate in our core. However, a point-by-point comparison of both records shows that they are not totally equivalent (Pearson's correlation coefficient  $R = 0.67$ , Fig. 6). This is not surprising since RAR values exclude all opal particles smaller than 45  $\mu\text{m}$  (our sieve mesh size), and fragments or opal produced by diatoms and sponge spicules are both considered as significant components of total opal (Leinen, 1985).

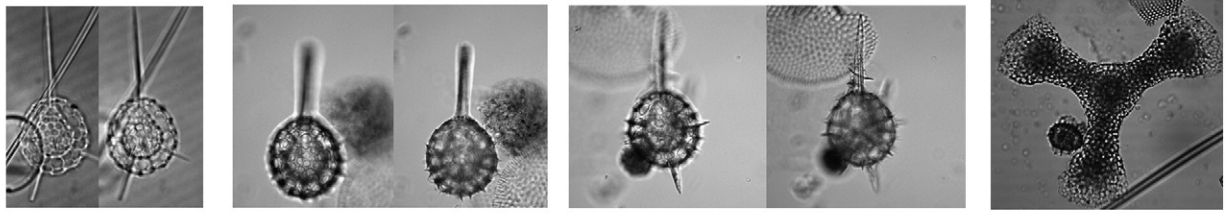
RAR and opal AR signals co-vary in accordance with the climatic background (Fig. 3C), in a way similar to contemporary conditions. Today, the Reykjanes Ridge area located southeast of the AF, has an annual mean sea surface temperature of 9°–10 °C, and is an area of maximal accumulation of radiolarian skeletons (up to 30,000 individuals per gram of sediment) in surface sediments from the North Atlantic region (Goll and Björklund, 1971; Matul, 1989a). Hence, we can assume that the samples with the highest radiolarian productivity in our study were similarly located south of the AF or near the region of mixing between the warm Atlantic and cold Arctic waters, as suggested by Molina-Cruz and Bernal-Ramirez (1996). Moreover, according to Aksu and Mudie (1985), high dissolved silica fluxes from the Arctic Ocean (Codispoti, 1979) and increased SST in the North Atlantic during interglacial stages would increase radiolarian and diatom production as well the preservation of opal in the sedimentary record (Berger, 1970; Takahashi, 1991; Nave et al., 2007).

#### Plate II.

- 1–3. *Druppactractus variabilis* Dumitrica, 1973. Hole B; core 9; section 2; cm 124–126 (77.84 mcd).  
 4. *Dictyocoryne profunda* Ehrenberg, 1860. Hole C; core 8; section 5; cm 2–4 (73.42 mcd).  
 5–6. *Heliodiscus asteriscus* Haeckel, 1887. Hole B; core 7; section 6; cm 38–40 (61.88 mcd).  
 7–8. *Larcopyle buetschlii* Dreyer, 1889. 7. Hole C; core 8; section 2; cm 146–148 (70.36 mcd). 8. Hole B; core 9; section 2; cm 124–126 (77.84 mcd).  
 9–14. *Larcopyle weddellium* Lazarus et al., 2005. Hole C; core 8; section 2; cm 146–148 (70.36 mcd).  
 15–19. *Larcospira minor* (Jørgensen, 1900). 15. Hole B; core 9; section 2; cm 124–126 (77.84 mcd). 16–19. Hole C; core 8; section 2; cm 146–148 (70.36 mcd).

#### Plate III. (see on page 62)

- 1–5. *Phorticium clevei* (Jørgensen, 1900). Hole C; core 8; section 4; cm 98–100 (72.88 mcd).  
 6–9. *Porodiscus* sp. 1. Hole C; core 8; section 4; cm 98–100 (72.88 mcd).  
 10. *Spongocore puella* Haeckel, 1887. Hole C; core 7; section 5; cm 146–148 (64.46 mcd).  
 11–12. *Spongodiscus* sp. Takahashi and Honjo, 1981. Hole C; core 8; section 2; cm 146–148 (70.36 mcd).  
 13–15. *Spongopyle osculosa* Dreyer, 1889. 13–14. Hole C; core 8; section 2; cm 146–148 (70.36 mcd). 15. Hole C; core 7; section 5; cm 146–148 (64.46 mcd).  
 16–19. *Spongotrochus glacialis* group Popofsky, 1908. Hole C; core 8; section 4; cm 98–100 (72.88 mcd).  
 20. *Stylatractus* sp. 1. Hole C; core 7; section 5; cm 146–148 (64.46 mcd).

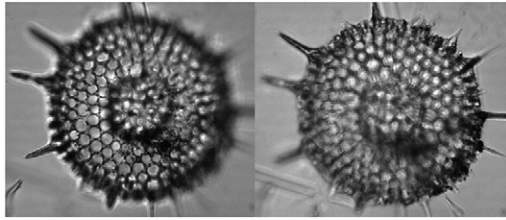


1

2

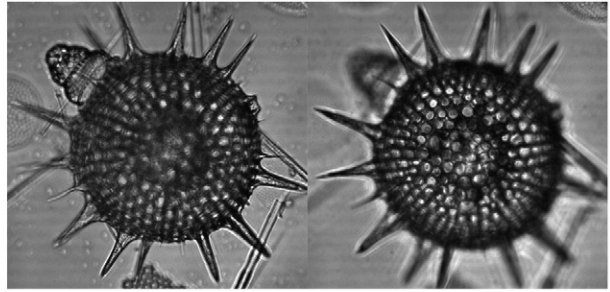
3

4



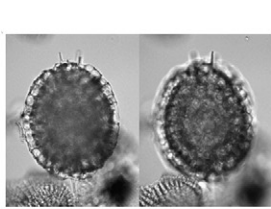
5

6



7

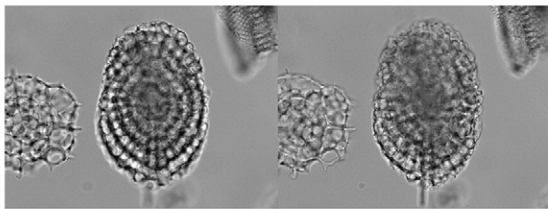
8



9

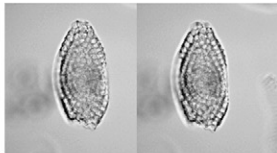
10

11



12

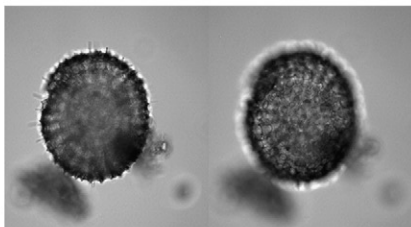
13



14

15

16



17

18

19

100  $\mu$ m

Plate II.

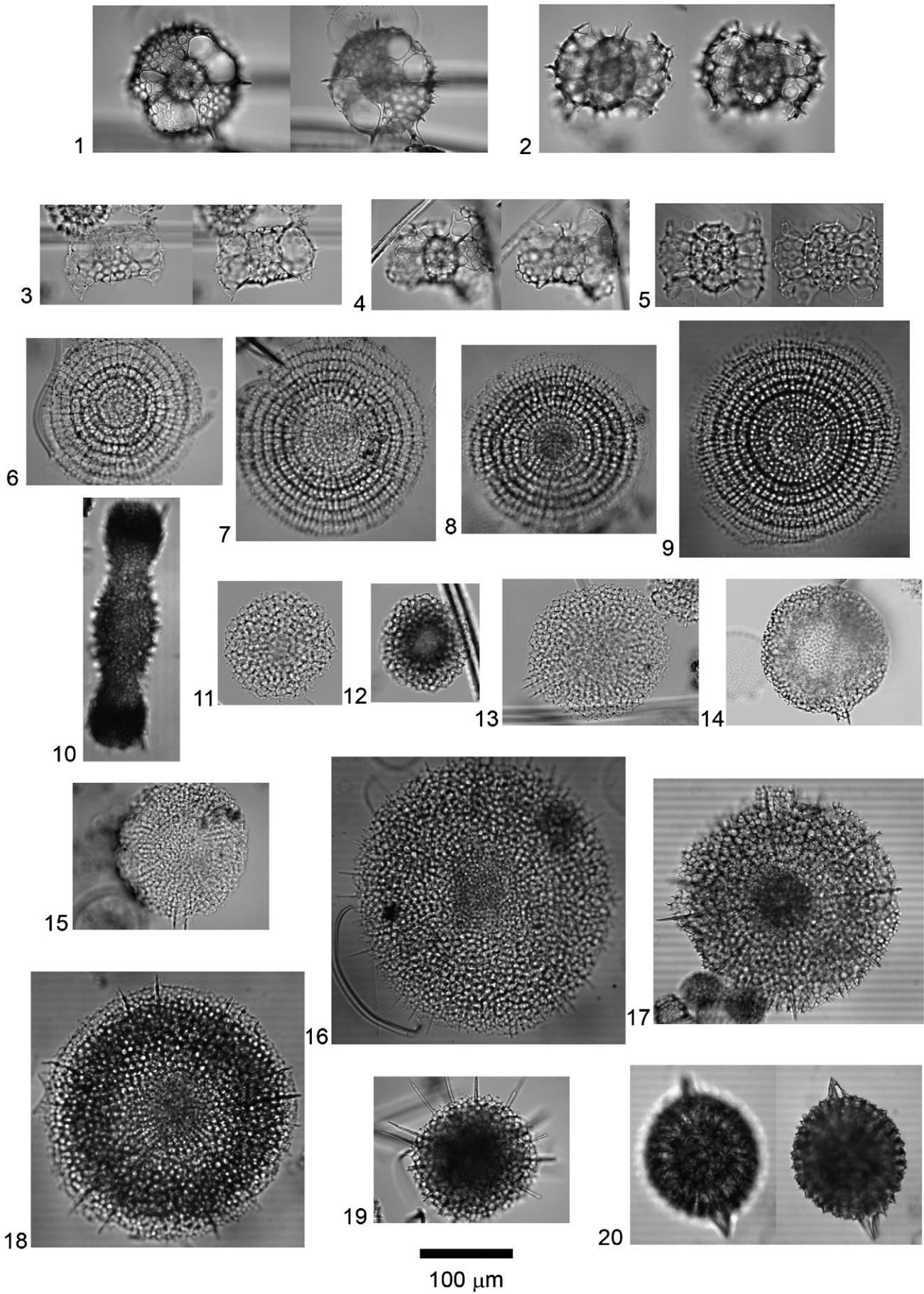
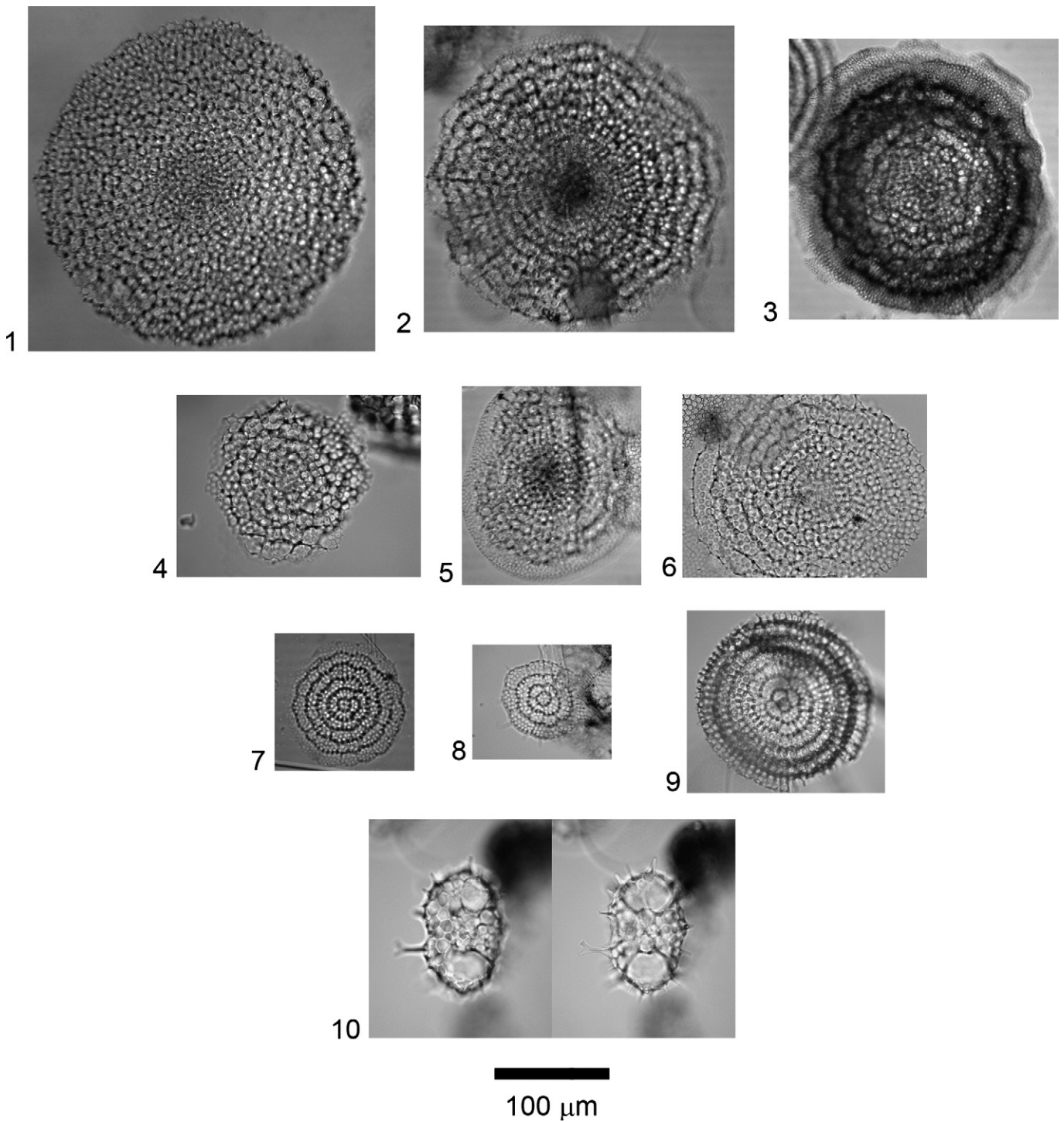


Plate III (see caption on page 60).



**Plate IV.**

- 1–6. *Stylochlamydidium venustum* (Bailey, 1856). 1–3. Hole C; core 8; section 2; cm 146–148 (70.36 mcd). 4–6. Hole C; core 8; section 4; cm 98–100 (72.88 mcd).  
 7–9. *Stylodictya validispina* Jørgensen, 1905. 7–8. Hole C; core 7; section 5; cm 146–148 (64.46 mcd). 9. Hole C; core 8; section 4; cm 98–100 (72.88 mcd).  
 10. *Tetrapyle octacantha* Müller, 1858. Hole C; core 8; section 2; cm 146–148 (70.36 mcd).

During IRD peaks, radiolarian shells are scarce indicating a period with decreased fertility in the upper water layers (Takahashi, 1991; Herguera, 1992). We interpret this as reduced opal and radiolarian production rates associated with the climate-induced southward migration of the AF, bringing to the Site U1314 location water with low SST, as well as reduced light due to extended ice cover, and

accompanying stratification by melt-water input (Morley, 1983; Aksu et al., 1992; Scharek et al., 1994). Additionally, transfer of Arctic waters rich in dissolved silica to the North Atlantic would be restricted due to the partial or total freezing of the Arctic Ocean, limiting nutrient input to the Site U1314 area (Aksu and Mudie, 1985). These results are in agreement with those of Thomas et al.

(1995) and Nave et al. (2007), who reported similar reduced surface productivity during Heinrich Events in the North Atlantic (50°–62° N), on the basis of benthic foraminifera and diatom-based proxies, respectively. Under these unfavorable environmental conditions, only cold-adapted radiolarian species like *C. davisiana* can survive (Morley, 1983; Morley and Hays, 1983; Morley et al., 1987; Bjørklund and Ciesielski, 1994). RAR are considerably low during these periods, and *C. davisiana* is not an important opal carrier (Jacot Des Combes and Abelmann, 2009), what explain the low opal AR values during critical glacial periods. Opal production was likely restricted to short periods in ice-free areas of the North Atlantic and Nordic Seas during summer (Pflaumann et al., 2003), similar to biological productivity episodes in the modern Arctic Ocean (Bjørklund and Kruglikova, 2003; Itaki, 2003).

Important reductions in the radiolarian content during glacial times since 950 ka, were also observed in the Northwest Pacific (Morley and Dworetzky, 1991). This suggests a cooling trend and onset of major ice-sheets that could have diminished glacial ocean productivity in the Northern Hemisphere (Berger et al., 1993; Berger and Jansen, 1994).

Additionally, since the Gardar Drift is a contourite drift formed by accumulation of sediment carried by the northeastern branch of the NADW, the ISOW (Bianchi and McCave, 2000), we can expect some size-sorting by bottom currents at Site U1314. Interglacial stages with low benthic  $\delta^{18}\text{O}$  values and null IRD deposition at Site U1314 correspond with periods of enhanced ventilation of the deep North Atlantic, as indicated the high benthic  $\delta^{13}\text{C}$  values ISOW, correspond with higher opal plankton productivity (Fig. 3A–C). Episodes of enhanced ISOW flow correspond with enhanced silt and clay deposition over the southern end of Gardar Drift (Bianchi and McCave, 1999). Hence, we suggest that increases of RAR and opal AR during interglacial periods are the result of enhanced transport of fine sediment by ISOW, being this material dominated biogenic particles derived of increased planktonic productivity in surface warmer waters. In contrast, during cold periods with weakened ISOW flow because of melt-water input at deep-convection sites, fine biogenic sedimentation was strongly diluted by periodic and episodic influxes of ice-rafted material from the surrounding land masses. Thus, the pronounced contrast in RAR and opal AR within G-IG stages results from oceanic circulation changes: either from surface circulation governing the ice-rafted detritus supplies and the planktonic biogenic production; and from deep circulation changes with the reactivation of the ISOW flow.

#### 5.4. Mid-Pleistocene Transition: impact on the radiolarian fauna

The interval investigated is within the period known as the Mid-Pleistocene Transition (MPT), characterized by a shift of global glacial/interglacial cycles from 41-kyr to 100-kyr (e.g. Ruddiman et al., 1989; Berger and Jansen, 1994). This shift in the dominant cyclicity triggered several large-scale climatic-events; e.g. global ice mass increase (Mudelsee and Schulz, 1997), drastic cooling and aridification in Africa (deMenocal, 1995), and large ice-sheet advances in the North and South Atlantic Ocean (Raymo et al., 1997; Ferretti et al., 2005). Likewise, clear radiolarian-based evidence shows change in the sea-surface temperature after MIS 26 toward cooler conditions (Morley and Dworetzky, 1991; Wang et al., 2000; Wang and Abelmann, 2002; Matul et al., 2009). According to faunal and isotopic data from Site U1314, we have identified two time-periods in our sedimentary record with different dominant cycles.

In the period from 1069 to 860 ka, the distribution of the RAR was characterized by frequent low-amplitude fluctuations (Fig. 3C), where adverse surface conditions (extensive sea-ice and IRD discharges) were not always accompanied by minimum values of radiolarian abundance and diversity, suggesting milder conditions, or an ocean that was only seasonally partly ice-covered and allowed a certain amount of plankton productivity. This interval is characterized by a radiolarian assemblage continuously dominated by the cold and deep-dweller *C. davisiana* (27% on average) (Fig. 4A), but co-occurring with shallow-dwellers, like *P. gracilipes* and *L. setosa* (Fig. 4F–G). The planktonic fauna and flora suggests a cold environment with relatively stable water masses at Site U1314, even during interglacials, as a result of an AF that was southward of its present position. Dominance (>60%) of the cold-water diatom *Neodenticula seminae* (Shimada et al., 2008) and high concentrations of  $\text{C}_{37:4}$  alkenones (McClymont et al., 2008) in the North Atlantic until MIS 21 support the inference made from our radiolarian data that cooler and fresher waters prevailed at Site U1314 during this interval. This also indicates the absence of extreme contrast between glacial and interglacial periods, due to the rapid fluctuation of the volume of continental ice-masses discharged to the North Atlantic following the 41-kyr Milankovitch obliquity cycles, without the time necessary for building up a great continental ice-sheet (Mudelsee and Schulz, 1997).

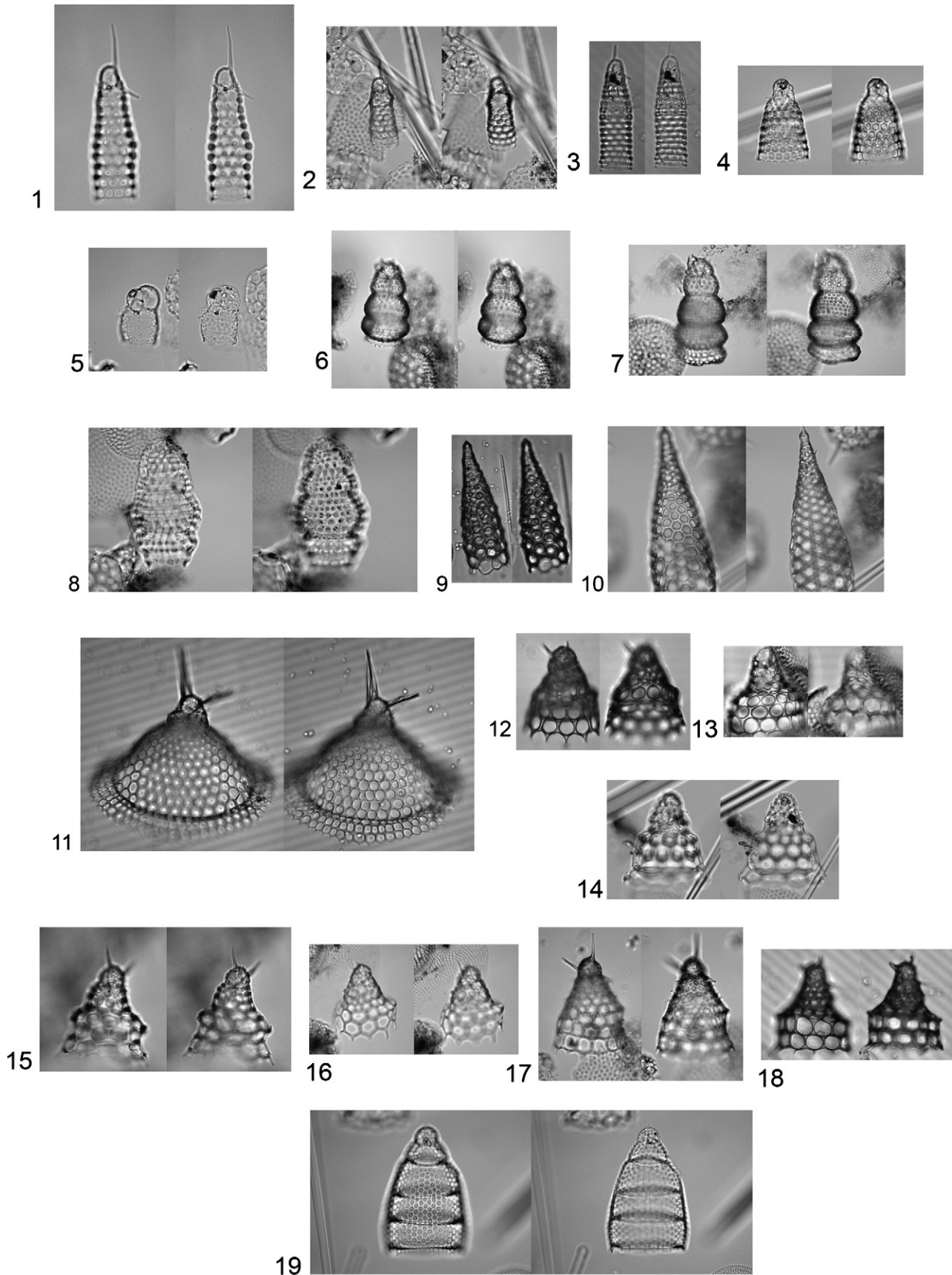
After ~860 ka ago, higher amplitude changes are recorded in the benthic  $\delta^{18}\text{O}$  signal. MIS 22 represents the first interval of substantial sea-level fall due to the glacioeustatic effect of continental ice

#### Plate V.

- 1–3. *Artostrobos annulatus* (Bailey, 1856). 1. Hole C; core 8; section 2; cm 146–148 (70.36 mcd). 2–3. Hole C; core 8; section 5; cm 2–4 (73.42 mcd).
4. *Artostrobos joergenseni* Petrushevskaya, 1967. Hole C; core 8; section 4; cm 98–100 (72.88 mcd).
5. *Botryocampe inflata* (Bailey, 1856). Hole C; core 8; section 5; cm 2–4 (73.42 mcd).
- 6–7. *Botryostrobos auritus/australis* (Ehrenberg) group Nigrini, 1977. Hole B; core 9; section 2; cm 124–126 (77.84 mcd).
8. *Botryostrobos tumidulus* (Bailey, 1856). Hole C; core 7; section 5; cm 146–148 (64.46 mcd).
- 9–10. *Cornutella profunda* Ehrenberg, 1854. Hole C; core 8; section 4; cm 98–100 (72.88 mcd).
11. *Corocalyptra craspedota* (Jørgensen, 1900). Hole A; core 8; section 6; cm 2–4 (69.17 mcd).
- 12–18. *Cycladophora davisiana* (Ehrenberg, 1862). 12–16. Hole B; core 9; section 2; cm 124–126 (77.84 mcd). 17–18. Hole C; core 8; section 2; cm 146–148 (70.36 mcd).
19. *Eucyrtidium acuminatum* (Ehrenberg, 1844). Hole C; core 8; section 4; cm 98–100 (72.88 mcd).

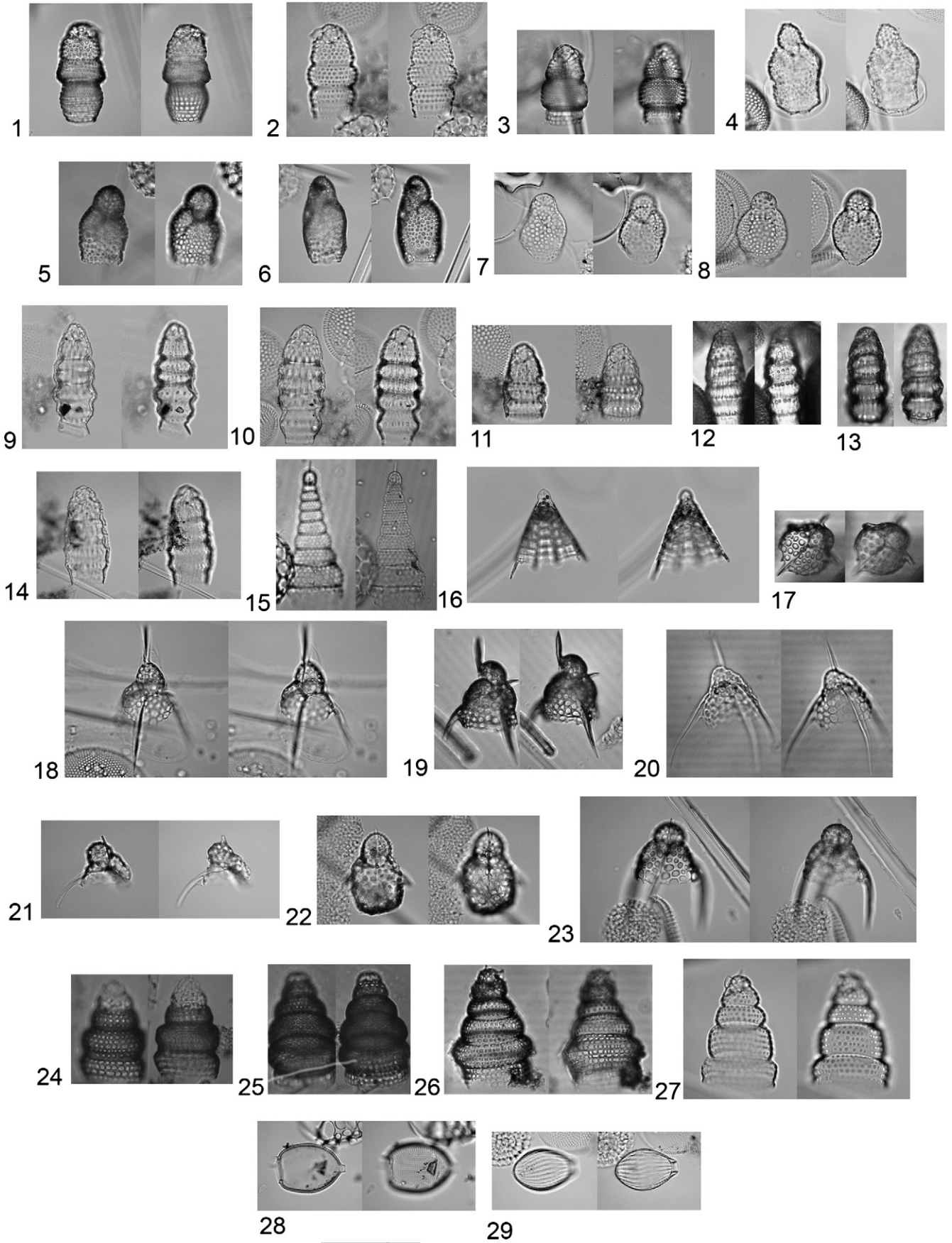
#### Plate VI. (see on page 66)

- 1–3. *Lithocampe platycephala* (Ehrenberg, 1873). Hole C; core 8; section 4; cm 98–100 (72.88 mcd).
- 4–8. *Lithomelissa setosa* Jørgensen, 1900. 4–6. Hole C; core 8; section 2; cm 146–148 (70.36 mcd). 7–8. Hole C; core 8; section 4; cm 98–100 (72.88 mcd).
- 9–14. *Lithomitra lineata/arachnea* group (Ehrenberg, 1839). 9. Hole C; core 8; section 2; cm 146–148 (70.36 mcd). 10–14. Hole C; core 7; section 5; cm 146–148 (64.46 mcd).
15. *Lithostrobos cuspidatus* (Bailey, 1856). Hole B; core 9; section 1; cm 126–128 (76.36 mcd).
16. *Periphyramis circumtexta* Haeckel, 1887. Hole C; core 8; section 2; cm 146–148 (70.36 mcd).
- 17–23. *Pseudodictyophimus gracilipes* (Bailey, 1856). 17–19. Hole C; core 8; section 5; cm 2–4 (73.42 mcd). 20–23. Hole C; core 8; section 5; cm 2–4 (73.42 mcd).
- 24–27. *Stichocorys seriata* Jørgensen, 1905. Hole C; core 8; section 4; cm 98–100 (72.88 mcd).
28. *Euphysetta nathorstii* Cleve, 1899. Hole C; core 8; section 4; cm 98–100 (72.88 mcd).
29. *Lirella melo* (Cleve, 1899). Hole C; core 8; section 2; cm 146–148 (70.36 mcd).



100  $\mu\text{m}$

Plate V.



100 μm

Plate VI (see caption on page 64).

build-up (Ferretti et al., 2005), consistent with the onset of the larger-amplitude 100-kyr Milankovitch eccentricity cycles during the Brunhes Chron (Mudelsee and Schulz, 1997). At Site U1314, the onset of the large-amplitude 100 ka cycles is manifested in the heavy benthic isotope values recorded during MIS 22, the highest for the last 1.1 Myr, and the massive growth of the ice rafting activity (Fig. 3A, E) suggests more severe glacial conditions. Glacial MIS 22 also represents a marked decrease in the accumulation of radiolarians, producing a greater contrast in glacial/interglacial planktonic production.

Likewise, a shift in the faunal composition can also be appreciated from about 850 ka upward. Upcore of MIS 21, the main cold taxon, *C. davisiana* underwent a large shift toward lower values (9% on average), while Shimada et al. (2008) observed a rapid disappearance of *N. seminae* from the North Atlantic diatom community, indicating an increase in the abundance of warm water diatoms. This scenario suggests a progressive northwest retreat of the AF, that culminated after 610 ka (MIS 16), to almost the same position that it occupies today (Wright and Flower, 2002), and hence an intensification of the northward flow of warm subtropical water, as reflected by the increased numbers of warm-water radiolarian species (e.g. Fig. 4I) after 850 ka. Moreover, higher opal and RAR values (Fig. 3C) after MIS 22 may indicate increased nutrient supply from land and continental shelves (Kitamura and Kawagoe, 2006) during large amplitude sea level fluctuations in glacial cycles after 890 ka (up to 33 m) (Prell, 1982; Ruddiman et al., 1989), leading to higher primary productivity (Broecker, 1982) and more efficient export flux of surface biosiliceous production (Shimada et al., 2008).

### 5.5. Diversity Index

Radiolarian diversity tracks decreasing ecosystem complexity with depth; in other words, there are more niches for radiolarians in shallow waters than in deep waters (McMillen and Casey, 1978). Hence, the *H* pattern at Site U1314 reflects water column “habitability”, which in turn depends on the climatic background. During interglacial periods, we observe numerous shallow water species, some of them microhervivores or with host-symbionts, such as *Didymocyrtis tetrathalamus*, *Eucyrtidium* spp., *Heliodiscus asteriscus*, *Peridium* sp., *Pterocanium praetextum*, *Tetrapyle octacantha* and *Ommatartus tetralamhus* (Takahashi et al., 2003). In contrast, during glacial periods, proliferation of shallow dwellers is hampered by harsh conditions such as sea ice and large salinity and temperature changes (Morley and Hays, 1983; Hays and Morley, 2003), leading to enhancement of percentages of the deep-dweller *C. davisiana*, which feeds mainly on phytodetritus provided by the brine pump system (Anderson, 1983; Abelmann and Nimmergut, 2005; Itaki et al., 2009). These results agree with the findings of Bjørklund et al. (1998) for the GIN Seas, who described the highest species richness for polycystine radiolarians in the warm Atlantic domain, while the lowest species number was found in the colder Arctic and polar domains. In the same way, the *H* pattern of radiolarians in the North Atlantic is very similar to that described by planktonic foraminifera: showing higher *H* values with the shifting of the warm Gulf Stream surface currents into the North Atlantic (Ruddiman, 1969; Balsam and Flessa, 1978) (Plates 1–6).

### 5.6. Time series and variance spectra

In order to show the dominant signals controlling the radiolarian assemblage structure, RAR, and opal AR, different techniques of spectral analysis (see Results) were used to study the variability of the three paleoceanographic records.

A prominent peak at 40 samples indicates a recurrence of taxa over a 7 kyr period (Fig. 8A). The power spectrum generated from the discrete Fourier transform of the Mantel correlogram shows two spectral peaks, at 6 and 14, reflecting an obliquity-dominated

(~48 kyr) and precessional signal (~20 kyr) over the 289 kyr period, respectively (Fig. 8B). The offset of 7 kyr in the obliquity frequency found in the radiolarian assemblage indicates that this spectral peak may not be related in a simple direct way to the suggested periodicity, and that further considerations which we have not identified in this study may influence the radiolarian assemblage periodicity. Likewise, spectral analysis of the RAR and opal AR record reveals a significant obliquity-related response (~45 kyr and ~47 kyr respectively) and precessional signal (~23 kyr and ~27 kyr respectively) (Fig. 8C–D). Therefore, frequencies driving RAR, opal AR and radiolarian assemblage signals coincide with the dominant Earth's solar orbit during the MPT, obliquity and precession (Mudelsee and Schulz, 1997; Mudelsee and Statterger, 1997), and indicating that the quasi-periodic oscillations observed in the variations of all bio-silica records at Site U1314 are largely controlled by these orbital parameters. Moreover, the periodogram from the RAR record also shows a third dominant cyclicity (~100 kyr) (Fig. 8C), and opal AR shows cyclicity centered at ~121 kyr and ~83 kyr (Fig. 8D), both related to eccentricity and reflecting the incipient climatic transformation at the MPT (Berger et al., 1993). Coherence between the dominant periodicity of the bio-silica records from Site U1314 indicates that climate changes driven by orbital parameters affect indistinctively the radiolarian group and all other opaline siliceous organisms (e.g. diatoms, silicoflagellates and sponge spicules), independently of their different ecologies.

## 6. Conclusions

The biogenic silica data set from Site U1314 provides a detailed record of surface oceanographic conditions (radiolarian assemblages) and surface productivity conditions (biogenic silica deposition) for the Early and Mid-Pleistocene (1069–779 ka) in the North Atlantic.

Temporal evolution of radiolarian assemblage composition and results from DCA show that the hydrographic and climatic context had a major influence on the radiolarian assemblage, yielding a clear glacial/interglacial faunal succession. During glacial periods *C. davisiana* dominated the radiolarian fauna because of the relatively low-surface temperatures and the episodically low surface salinities caused by ice melting and the increase in the IRD delivery, which restricted the radiolarian productivity and diversity (*H*). In contrast, during interglacial periods, warm and shallow water dwellers (e.g. *P. gracilipes*, *L. setosa*, *S. glacialis/resurgens* group and *S. venustum*) proliferate due to the open water conditions provided by the vicinity of the warm Atlantic waters and the ice-sheet retreat, which is conducive to higher surface water productivity and higher *H*. Furthermore, occasional occurrence of species with tropical-subtropical affinity (“drift fauna group”) is related to a northeastward transport by the warm Atlantic surface waters to the Site U1314 position; therefore do not represent “in-situ” production.

The temporal pattern of the RAR runs parallel with the DI and opal AR patterns, suggesting that radiolarians as a whole can be considered a productivity indicator in Pleistocene samples of the North Atlantic. Radiolarian and opal paleofluxes show significant fluctuations along the sedimentary record according to the climate-induced latitudinal migration of the AF and associated changes that took place in the water column; increased RAR and opal values during interglacials indicate intense water mixing and active NAC flow in the North Atlantic, that decrease during glacial periods, when severe surface conditions (low SST and sea-ice cover) and stratification by melt-water input during ice-rafting episodes occurred.

Additionally, bottom currents play an important role on fine grain material sedimentation at Site U1314. Enhanced ISOW flow during interglacial periods results in an increase in accumulation of fine biogenic particles produced at surface, while less vigorous deep-water flow over Gardar Drift during melt-water events transported and accumulated less fine-grained material, including less opal plankton,

that led to the relative concentration in the sediment of the coarsed-grained fraction. Therefore, the pronounced contrast in RAR and opal AR within G-IG stages results from a combination of surface and deep oceanic circulation changes: either from surface circulation governing the ice-rattened detritus supplies and the planktonic biogenic production; and from deep circulation changes with the reactivation of the ISOW flow.

The temporal variation of the radiolarian assemblage along the Site U1314 record shows a drastic change at MIS 22 (~860 ka). Before this time the deep-dwelling taxon *C. davisiana* co-existed with shallow dwellers, e.g. *P. gracilipes* and *L. setosa*, indicating a milder environment without such extreme seasonal conditions and not so severe glacial conditions, with dominance of the 41-kyr glacial cyclicity. Since ~860 ka more severe glacial conditions, due to increased global ice-volume, caused a strong reduction in the North Atlantic thermohaline circulation (Mudelsee and Statterger, 1997). Isotopic and faunal records at Site U1314 do show higher amplitude variations in response to these new environmental conditions. The radiolarian assemblage shows a higher contrast between glacial and interglacial periods. Cold and deep-dwellers dominated during glacial periods and IRD discharge. In contrast, interglacial periods are characterized by an increase in shallow-dwellers that represent enhanced opal and radiolarian production during introduction of warm Atlantic waters and water mixing.

Spectral analyses (Mantel periodograms) of the radiolarian assemblage reveal dominant periodicities of ~48 kyr and ~20 kyr, which could be related to the Milankovitch cycles of obliquity and precession, respectively dominant during the MPT. RAR and opal AR records exhibit a coherent response to the whole radiolarian assemblage, with a more significant obliquity and precessional-related cyclicity, and showing an incipient eccentricity signal, which represents the prelude of the high-amplitude cycles typical during the Late Pleistocene.

Supplementary materials related to this article can be found online at [doi:10.1016/j.palaeo.2011.05.049](https://doi.org/10.1016/j.palaeo.2011.05.049).

## Acknowledgements

This work was funded by Ministerio de Ciencia e Innovación Project GRACCIE (CONSOLIDER-INGENIO CSD 2007-00067) and CGL2008-05560/BTE as well as Junta de Castilla y Leon Grupo GR34, and by a MEC FPI Grant to Iván Hernández-Almeida (BES-2006-12787). We are grateful to Øyvind Hammer for his critical review comments on this manuscript. His many discussions of statistical approaches, help and suggestions greatly improved on this work and are appreciated. Stan Kling is thanked for his review and linguistic corrections of the manuscript. Also Dr. Richard Benson and one anonymous reviewer provided valuable comments. The senior author is also thankful for the support that was provided by the Natural History Museum, University of Oslo, during the preparation of this paper. This research used samples from IODP Expedition 306.

## References

- Abelmann, A., Gowing, M.M., 1997. Spatial distribution pattern of living polycystine radiolarian taxa—baseline study for paleoenvironmental reconstructions in the Southern Ocean (Atlantic sector). *Marine Micropaleontology* 30 (1–3), 3–28.
- Abelmann, A., Nimmergut, A., 2005. Radiolarians in the Sea of Okhotsk and their ecological implication for paleoenvironmental reconstructions. *Deep Sea Research Part II: Topical Studies in Oceanography* 52 (16–18), 2302–2331.
- Aksu, A.E., Mudie, P.J., 1985. Late Quaternary stratigraphy and paleoecology of northwest Labrador Sea. *Marine Micropaleontology* 9 (6), 537–557.
- Aksu, A.E., Mudie, P.J., de Vernal, A., Gillespie, H., 1992. Ocean-atmosphere responses to climatic change in the Labrador Sea: Pleistocene plankton and pollen records. *Palaeogeography, Palaeoclimatology, Palaeoecology* 92 (1–2), 121–138.
- Alley, R.B., MacAyeal, D.R., 1994. Ice-rafted debris associated with binge/purge oscillations of the Laurentide Ice Sheet. *Paleoceanography* 9 (4), 503–511.
- Anderson, O.R., 1983. *Radiolaria*. Springer, New York. 355 pp.
- Balsam, W.L., Flessa, K.W., 1978. Patterns of planktonic foraminiferal abundance and diversity in surface sediments of the western North Atlantic. *Marine Micropaleontology* 3 (3), 279–294.
- Benson, R.N., 1972. Radiolaria, Leg XII, Deep Sea Drilling Project. In: Laughton, A.S., et al. (Ed.), *Initial Reports of the Deep Sea Drilling Project*. U.S. Government Printing Office, Washington, D.C, pp. 1085–1113.
- Berger, W.H., 1970. Biogenous deep-sea sediments: fractionation by deep-sea circulation. *Geological Society of America Bulletin* 81 (5), 1385–1402.
- Berger, W.H., Jansen, E., 1994. Mid-Pleistocene climate shift: the Nansen connection. In: Johannessen, O.D., Muench, R.D., Overland, J.E. (Eds.), *The Polar Oceans and Their Role in Shaping the Global Environment: The Nansen Centennial Volume*. : AGU, Geophysical Monographs. AGU, Washington, D.C, pp. 295–311.
- Berger, W.H., Bickert, T., Jansen, E., Wefer, G., Yasuda, M., 1993. The central mystery of the Quaternary Ice Age. *Oceanus* 36, 53–56.
- Bianchi, G.G., McCave, I.N., 1999. Holocene periodicity in North Atlantic climate and deep-ocean flow south of Iceland. *Nature* 397 (6719), 515–517.
- Bianchi, G.G., McCave, I.N., 2000. Hydrography and sedimentation under the deep western boundary current on Björn and Gardar Drifts, Iceland Basin. *Marine Geology* 165 (1–4), 137–169.
- Björklund, K.R., Ciesielski, P.F., 1994. Ecology, morphology, stratigraphy, and the paleoceanographic significance of *Cycladophora davisiana davisiana*. Part I: Ecology and morphology. *Marine Micropaleontology* 24 (1), 71–88.
- Björklund, K.R., Kruglikova, S.B., 2003. Polycystine radiolarians in surface sediments in the Arctic Ocean basins and marginal seas. *Marine Micropaleontology* 49 (3), 231–273.
- Björklund, K.R., Cortese, G., Swanberg, N., Schrader, H.J., 1998. Radiolarian faunal provinces in surface sediments of the Greenland, Iceland and Norwegian (GIN) Seas. *Marine Micropaleontology* 35 (1–2), 105–140.
- Boltovskoy, D., Alder, V.A., Abelmann, A., 1993. Radiolarian sedimentary imprint in Atlantic equatorial sediments: comparison with the yearly flux at 853 m. *Marine Micropaleontology* 23 (1), 1–12.
- Boltovskoy, D., Uliana, E., Wefer, G., 1996. Seasonal variation in the flux of microplankton and radiolarian assemblage compositions in the Northeastern tropical Atlantic at 2,195 m. *Limnology and Oceanography* 41 (4), 615–635.
- Bond, G.C., Lott, R., 1995. Iceberg discharges into the North Atlantic on millennial time scales during the last glaciation. *Science* 267 (5200), 1005–1010.
- Bond, G., et al., 1992. Evidence for massive discharges of icebergs into the North Atlantic Ocean during the last glacial period. *Nature* 360, 245–249.
- Broecker, W.S., 1982. Ocean chemistry during glacial time. *Geochimica et Cosmochimica Acta* 46 (10), 1689–1705.
- Broecker, W.S., Peng, T.H., 1982. *Tracers in the Sea*. Eldigio Press, Palisades, N.Y.
- Broecker, W., Bond, G., Klas, M., Clark, E., McManus, J., 1992. Origin of the northern Atlantic's Heinrich events. *Climate Dynamics* 6 (3), 265–273.
- Casey, R.E., et al., 1979. Radiolarian ecology and the development of the radiolarian component in Holocene sediments, Gulf of Mexico and adjacent seas with potential paleontological applications. *Transactions of the Gulf Coast Association of Geological Societies* 29, 228–237.
- Channell, J.E.T., et al., 2006. Site U1314 Summary. In: Channell, J.E.T., et al. (Ed.), *Proc. IODP, 303/306. Integrated Ocean Drilling Program Management International, Inc., College Station TX*.
- Ciesielski, P.F., Björklund, K.R., 1995. Ecology, morphology, stratigraphy, and the paleoceanographic significance of *Cycladophora davisiana davisiana*. Part II: Stratigraphy in the North Atlantic (DSDP Site 609) and Labrador Sea (ODP Site 646B). *Marine Micropaleontology* 25 (1), 67–86.
- Codispoti, L.A., 1979. Arctic Ocean processes in relation to the dissolved silicon content of the Atlantic. *Marine Science Communications* 5 (6), 361–381.
- Coplen, T.B., 1996. More uncertainty than necessary. *Paleoceanography* 11 (4), 369–370.
- Cortese, G., Björklund, K.R., Dolven, J.K., 2003. Polycystine radiolarians in the Greenland-Iceland-Norwegian Seas: species and assemblage distribution. *Sarsia* 88, 65–88.
- Cortese, G., Gersonde, R., Hillenbrand, C.-D., Kuhn, G., 2004. Opal sedimentation shifts in the World Ocean over the last 15 Myr. *Earth and Planetary Science Letters* 224 (3–4), 509–527.
- De Wever, P., Azéma, J., Fourcade, E., 1994. Radiolaires et radiolarites: productivité primaire, diagenèse et paléogéographie. *Bulletin des Centres de Recherches Exploration-Production Elf Aquitaine* 18 (1), 315–379.
- deMenocal, P.B., 1995. Plio-Pleistocene African climate. *Science* 270 (5233), 53–59.
- Dokken, T.M., Jansen, E., 1999. Rapid changes in the mechanism of ocean convection during the last glacial period. *Nature* 401 (6752), 458–461.
- Dow, R.L., 1978. Radiolarian distribution and the late pleistocene history of the Southeastern Indian Ocean. *Marine Micropaleontology* 3 (3), 203–227.
- Ferretti, P., Shackleton, N.J., Rio, D., Hall, M.A., 2005. Early-Middle Pleistocene deep circulation in the western subtropical Atlantic: southern hemisphere modulation of the North Atlantic Ocean. In: Head, M.J., Gibbard, P.L. (Eds.), *Early-Middle Pleistocene Transitions: The Land-Ocean Evidence*. Geological Society, London, pp. 131–145.
- Flower, B.P., et al., 2000. North Atlantic Intermediate to deep water circulation and chemical stratification during the past 1 Myr. *Paleoceanography* 15 (4), 388–403.
- Goll, R.M., Björklund, K.R., 1971. Radiolaria in surface sediments of the North Atlantic Ocean. *Micropaleontology* 17 (4), 434–454.
- Goll, R.M., Björklund, K.R., 1974. Radiolaria in surface sediments of the South Atlantic. *Micropaleontology* 20 (1), 38–75.
- Hammer, Ø., 2007. Spectral analysis of a Plio-Pleistocene multispecies time series using the Mantel periodogram. *Palaeogeography, Palaeoclimatology, Palaeoecology* 243 (3–4), 373–377.
- Hammer, Ø., Harper, D.A.T., Ryan, P.D., 2001. PAST: Paleontological statistics software package for education and data analysis. *Palaeontologia Electronica* 4 (1).

- Haslett, S.K., 1995. Pliocene–Pleistocene radiolarian biostratigraphy and palaeoceanography of the North Atlantic. Geological Society, London, Special Publications 90 (1), 217–225.
- Hass, C., et al., 2001. The potential of synoptic plankton analyses for paleoclimatic investigations: five plankton groups from the Holocene Nordic Seas. In: Schäfer, P., Ritzrau, W., Schlüter, M., Thiede, J. (Eds.), *The Northern North Atlantic: A Changing Environment*. Springer, Berlin, pp. 291–318.
- Hatakeda, K., Björklund, K.R., 2009. Polycystine radiolarian assemblages from IODP Expedition 306 Site U1313 and Site U1314, a preliminary result. *News of Osaka Micropaleontologists, Special Volume*, 14, pp. 91–108.
- Hays, J.D., Morley, J.J., 2003. The Sea of Okhotsk: a window on the Ice Age Ocean. *Deep Sea Research Part I: Oceanographic Research Papers* 50 (12), 1481–1506.
- Head, M.J., Gibbard, P.L., 2005. Early–Middle Pleistocene transitions: an overview and recommendation for the defining boundary. Geological Society, London, Special Publications 247 (1), 1–18.
- Heinrich, H., 1988. Origin and consequences of cyclic ice rafting in the Northeast Atlantic Ocean during the past 130,000 years. *Quaternary Research* 29 (2), 142–152.
- Hemming, S.R., 2004. Heinrich events: massive late Pleistocene detritus layers of the North Atlantic and their global climate imprint. *Rev. Geophys.* 42, RG1005.
- Herguera, J.C., 1992. Deep-sea benthic foraminifera and biogenic opal: glacial to postglacial productivity changes in the western equatorial Pacific. *Marine Micropaleontology* 19 (1–2), 79–98.
- Hernández-Almeida, I., Sierro, F.J., Cacho, I. and Flores, J.A., in preparation. Impact of suborbital climate changes in the North Atlantic on ice-sheets dynamics at the Mid-Pleistocene Transition.
- Imbrie, J., Kipp, N.G., 1971. A new micropaleontological method for quantitative paleoclimatology. Application to a late Pleistocene Caribbean core. In: Turekian, K.K. (Ed.), *The Late Cenozoic Glacial Ages*. Yale University Press, New Haven, pp. 71–131.
- Itaki, T., 2003. Depth-related radiolarian assemblage in the water-column and surface sediments of the Japan Sea. *Marine Micropaleontology* 47 (3–4), 253–270.
- Itaki, T., Khim, B.-K., Ikehara, K., 2008. Last glacial–Holocene water structure in the southwestern Okhotsk Sea inferred from radiolarian assemblages. *Marine Micropaleontology* 67 (3–4), 191–215.
- Itaki, T., et al., 2009. Late Pleistocene stratigraphy and palaeoceanographic implications in northern Bering Sea slope sediments: evidence from the radiolarian species *Cycladophora davisiana*. *Journal of Quaternary Science* 24 (8), 856–865.
- Jacot Des Combes, H., Abelmann, A., 2009. From species abundance to opal input: simple geometrical models of radiolarian skeletons from the Atlantic sector of the Southern Ocean. *Deep Sea Research Part I: Oceanographic Research Papers* 56 (5), 757–771.
- Johannessen, T., Jansen, E., Flato, A., Ravelo, A.C., 1994. The relationship between surface water masses, oceanographic fronts and paleoclimatic proxies in surface sediments of the Greenland, Iceland, Norwegian seas. In: Zahn, R., Pedersen, T.F., Kaminski, M.A., Labeyrie, L. (Eds.), *Carbon Cycling in the Glacial Ocean: Constraints on the Oceans's Role in Global Change*. Springer-Verlag, Berlin, pp. 61–85.
- Kawagata, S., Hayward, B.W., Grenfell, H.R., Sabaa, A., 2005. Mid-Pleistocene extinction of deep-sea foraminifera in the North Atlantic Gateway (ODP sites 980 and 982). *Palaeogeography, Palaeoclimatology, Palaeoecology* 221 (3–4), 267–291.
- Kitamura, A., Kawagoe, T., 2006. Eustatic sea-level change at the Mid-Pleistocene climate transition: new evidence from the shallow-marine sediment record of Japan. *Quaternary Science Reviews* 25 (3–4), 323–335.
- Kleiven, H.F., Jansen, E., Curry, W.B., Hodell, D.A., Venz, K., 2003. Atlantic Ocean thermohaline circulation changes on orbital to suborbital timescales during the mid-Pleistocene. *Paleoceanography* 18.
- Kling, S.A., Boltovskoy, D., 1995. Radiolarian vertical distribution patterns across the Southern California current. *Deep Sea Research Part I: Oceanographic Research Papers* 42 (2), 191–231.
- Koç, N., Schrader, H., 1990. Surface sediment diatom distribution and Holocene paleotemperature variations in the Greenland, Iceland and Norwegian Sea. *Paleoceanography* 5 (4), 557–580.
- Koç, N., Jansen, E., Hafliðason, H., 1993. Paleoceanographic reconstructions of surface ocean conditions in the Greenland, Iceland and Norwegian seas through the last 14 ka based on diatoms. *Quaternary Science Reviews* 12 (2), 115–140.
- Koç, N., Hodell, D.A., Kleiven, H., Labeyrie, L., 1999. High-resolution Pleistocene diatom biostratigraphy of site 983 and correlations with isotope stratigraphy. In: Raymo, M.E., Jansen, E., Blum, P., Herbert, T.D. (Eds.), *Proceedings of the Ocean Drilling Program, Scientific Results*. Ocean Drilling Program, College Station, TX.
- Krauss, W., 1986. The North Atlantic Current. *J. Geophys. Res.* 91 (C4), 5061–5074.
- Leinen, M., 1985. Techniques for determining opal in deep-sea sediments: A comparison of radiolarian counts and X-ray diffraction data. *Marine Micropaleontology* 9 (5), 375–383.
- Lisiecki, L.E., Raymo, M.E., 2005. A Pliocene–Pleistocene stack of 57 globally distributed benthic  $\delta^{18}\text{O}$  records. *Paleoceanography* 20, PA1003.
- Lüer, V., 2003. Quaternary Radiolarians from Offshore Eastern New Zealand, Southwestern Pacific (ODP Leg 181, Site 1123): Importance for Correlation and Identification of Climatic Changes. University of Bremen, Bremen, 103 pp.
- Marchitto Jr., T.M., Oppo, D.W., Curry, W.B., 2002. Paired benthic foraminiferal Cd/Ca and Zn/Ca evidence for a greatly increased presence of Southern Ocean Water in the glacial North Atlantic. *Paleoceanography* 17 (3), 1038.
- Marino, M., Maiorano, P., Lirer, F., 2008. Changes in calcareous nannofossil assemblages during the Mid-Pleistocene Revolution. *Marine Micropaleontology* 69 (1), 70–90.
- Maslin, M.A., Shackleton, N.J., Pflaumann, U., 1995. Surface water temperature, salinity, and density changes in the Northeast Atlantic during the Last 45,000 Years: Heinrich Events, deep water formation, and climatic rebounds. *Paleoceanography* 10 (3), 527–544.
- Matul, A.G., 1989a. Radiolarian distribution in the surface sediment layer in the north Atlantic. *Oceanology* 29 (6), 992–998.
- Matul, A.G., 1989b. Radiolarian distribution in the surface sediment layer in the north Atlantic. *Oceanology* 29 (6), 992–998.
- Matul, A.G., 1994a. Late Quaternary paleoceanology of the North Atlantic based on radiolaria analysis data. *Oceanology* 34 (4), 550–555.
- Matul, A.G., 1994b. On the problem of paleoceanological evolution of the Reykjanes Ridge region (North Atlantic) during the last deglaciation based on the study of radiolarian. *Oceanology* 34 (6), 806–814.
- Matul, A.G., Yushina, I.G., 1999. Radiolarians in North Atlantic sediment. In: Spielhagen, R.F., Barash, M.S., Ivanov, G.L., Thiede, J. (Eds.), *German–Russian Cooperation: Biogeographic and Biostratigraphic Investigations on Selected Sediment Cores from the Eurasian Continental Margin and Marginal Seas to Analyze the Late Quaternary Climatic Variability*. Ber. Polarforsch.
- Matul, A., Yushina, I.G., Emelyanov, E.M., 2002. On the Late Quaternary paleohydrological parameters of the Labrador Sea based on radiolarians. *Oceanology* 42 (2), 262–266.
- Matul, A., Abelmann, A., Nürnberg, D., Tiedemann, R., 2009. Stratigraphy and major paleoenvironmental changes in the Sea of Okhotsk during the last million years inferred from radiolarian data. *Oceanology* 49 (1), 93–100.
- McClymont, E.L., Rosell-Melé, A., Haug, G.H., Lloyd, J.M., 2008. Expansion of subarctic water masses in the North Atlantic and Pacific oceans and implications for mid-Pleistocene ice sheet growth. *Paleoceanography* 23, PA4214.
- McIntyre, K., Ravelo, A.C., Delaney, M.L., 1999. North Atlantic intermediate waters in the Late Pliocene to Early Pleistocene. *Paleoceanography* 14 (3), 324–335.
- McManus, J.F., et al., 1994. High-resolution climate records from the North Atlantic during the last interglacial. *Nature* 371 (6495), 326–329.
- McManus, J.F., Oppo, D.W., Cullen, J.L., 1999. A 0.5-million-year record of millennial-scale climate variability in the North Atlantic. *Science* 283 (5404), 971–975.
- McMillen, K.J., Casey, R.E., 1978. Distribution of living polycystine radiolarians in the Gulf of Mexico and Caribbean Sea, and comparison with the sedimentary record. *Marine Micropaleontology* 3 (2), 121–145.
- Molina-Cruz, A., 1977. Radiolarian assemblages and their relationship to the oceanography of the subtropical southeastern Pacific. *Marine Micropaleontology* 2, 315–352.
- Molina-Cruz, A., 1988. Late Quaternary oceanography of the mouth of the Gulf of California: the polycystine connection. *Paleoceanography* 3 (4), 447–459.
- Molina-Cruz, A., 1991. Holocene palaeo-oceanography of the northern Iceland Sea, indicated by radiolaria and sponge spicules. *Journal of Quaternary Science* 6 (4), 303–312.
- Molina-Cruz, A., Bernal-Ramirez, R.G., 1996. Distribution of radiolaria in surface sediments and its relation to the oceanography of the Iceland and Greenland Seas. *Sarsia* 81, 315–328.
- Molina-Cruz, A., Welling, L., Caudillo-Bohorquez, A., 1999. Radiolarian distribution in the water column, southern Gulf of California, and its implication in thanatocoenose constitution. *Marine Micropaleontology* 37 (2), 149–171.
- Morley, J.J., 1983. Identification of density-stratified waters in the late-Pleistocene North Atlantic: a faunal derivation. *Quaternary Research* 20 (3), 374–386.
- Morley, J.J., Dworetzky, B.A., 1991. Evolving Pliocene–Pleistocene climate: a North Pacific perspective. *Quaternary Science Reviews* 10 (2–3), 225–237.
- Morley, J.J., Hays, J.D., 1979. *Cycladophora davisiana*: a stratigraphic tool for Pleistocene North Atlantic and interhemispheric correlation. *Earth and Planetary Science Letters* 44 (3), 383–389.
- Morley, J.J., Hays, J.D., 1983. Oceanographic conditions associated with high abundances of the radiolarian *Cycladophora davisiana*. *Earth and Planetary Science Letters* 66, 63–72.
- Morley, J.J., Hays, J.D., Robertson, J.H., 1982. Stratigraphic framework for the late Pleistocene in the northwest Pacific Ocean. *Deep Sea Research Part A: Oceanographic Research Papers* 29 (12), 1485–1499.
- Morley, J., Piasis, N., Leinen, M., 1987. Late Pleistocene time series of atmospheric and oceanic variables recorded in sediments from the Subarctic Pacific. *Paleoceanography* 2 (1), 49–62.
- Moros, M., et al., 2004. Sea surface temperatures and ice rafting in the Holocene North Atlantic: climate influences on northern Europe and Greenland. *Quaternary Science Reviews* 23 (20–22), 2113–2126.
- Mortlock, R.A., Froelich, P.N., 1989. A simple method for the rapid determination of biogenic opal in pelagic marine sediments. *Deep Sea Research Part A: Oceanographic Research Papers* 36 (9), 1415–1426.
- Mudelsee, M., Schulz, M., 1997. The Mid-Pleistocene climate transition: onset of 100 ka cycle lags ice volume build-up by 280 ka. *Earth and Planetary Science Letters* 151 (1–2), 117–123.
- Mudelsee, M., Statterger, K., 1997. Exploring the structure of the mid-Pleistocene revolution with advanced methods of time-series analysis. *Geologische Rundschau* 86 (2), 499–511.
- Nave, S., et al., 2007. Primary productivity response to Heinrich events in the North Atlantic Ocean and Norwegian Sea. *Paleoceanography* 22.
- Nimmergut, A., Abelmann, A., 2002. Spatial and seasonal changes of radiolarian standing stocks in the Sea of Okhotsk. *Deep Sea Research Part I: Oceanographic Research Papers* 49 (3), 463–493.
- Okazaki, Y., et al., 2003. Radiolarians under the seasonally sea-ice covered conditions in the Okhotsk Sea: flux and their implications for paleoceanography. *Marine Micropaleontology* 49 (3), 195–230.
- Okazaki, Y., Takahashi, K., Itaki, T., Kawasaki, Y., 2004. Comparison of radiolarian vertical distributions in the Okhotsk Sea near the Kuril Islands and in the northwestern North Pacific off Hokkaido Island. *Marine Micropaleontology* 51 (3–4), 257–284.
- Oppo, D., 1997. Millennial climate oscillations. *Science* 278 (5341), 1244–1246.
- Oppo, D.W., Lehman, S.J., 1993. Mid-depth circulation of the Subpolar North Atlantic during the Last Glacial Maximum. *Science* 259 (5098), 1148–1152.

- Oppo, D.W., Lehman, S.J., 1995. Suborbital timescale variability of North Atlantic Deep Water during the past 200,000 years. *Paleoceanography* 10 (5), 901–910.
- Paillard, D.L., Yiou, L.P., 1996. Macintosh program performs time-series analysis. *Eos Trans. AGU*, 77, p. 379.
- Petrushevskaya, M.G., 1971. Spumellarian and Nasselarian radiolaria in the plankton and bottom sediments of the Central Pacific. In: Funnel, B.M., Riedel, W.R. (Eds.), *Micropaleontology of Oceans*. Cambridge University Press, Cambridge, pp. 309–317.
- Petrushevskaya, M.G., Björklund, K.R., 1974. Radiolarians in Holocene sediments of the Norwegian-Greenland Seas. *Sarsia* 57 (4), 33–46.
- Pflaumann, U., et al., 2003. Glacial North Atlantic: sea-surface conditions reconstructed by GLAMAP 2000. *Paleoceanography* 18 (3), 1065.
- Pielou, E.C., 1975. *Ecological Diversity*. Wiley, New York, 165 pp.
- Prell, W.L., 1982. Oxygen and carbon isotope stratigraphy for the Quaternary of Hole 502B: evidence for two modes of isotopic variability. In: Prell, W.L., Gardner, J.L. (Eds.), *Initial Reports. Deep Sea Drilling Project*, pp. 455–464.
- Raymo, M.E., Nisancioglu, K., 2003. The 41 kyr world: Milankovitch's other unsolved mystery. *Paleoceanography* 18, 1011.
- Raymo, M.E., Oppo, D.W., Curry, W., 1997. The Mid-Pleistocene climate transition: a deep sea carbon isotopic perspective. *Paleoceanography* 12 (4), 546–559.
- Raymo, M.E., et al., 2004. Stability of North Atlantic water masses in face of pronounced climate variability during the Pleistocene. *Paleoceanography* 19, PA2008.
- Rogachev, K.A., 2000. Recent variability in the Pacific western subarctic boundary currents and Sea of Okhotsk. *Progress in Oceanography* 47 (2–4), 299–336.
- Ruddiman, W.F., 1969. Recent planktonic Foraminifera: dominance and diversity in North Atlantic surface sediments. *Science* 164 (3884), 1164–1167.
- Ruddiman, W.F., 1977. Late Quaternary deposition of ice-rafted sand in the subpolar North Atlantic (lat 40° to 65°N). *Geological Society of America Bulletin* 88 (12), 1813–1827.
- Ruddiman, W.F., McIntyre, A., 1981. The mode and mechanism of the last deglaciation: oceanic evidence. *Quaternary Research* 16 (2), 125–134.
- Ruddiman, W.F., McIntyre, A., Niebler-Hunt, V., Durazzi, J.T., 1980. Oceanic evidence for the mechanism of rapid northern hemisphere glaciation. *Quaternary Research* 13 (1), 33–64.
- Ruddiman, W.F., Raymo, M.E., Martinson, D.G., Clement, B.M., Backman, J., 1989. Pleistocene evolution: Northern hemisphere ice sheets and North Atlantic Ocean. *Paleoceanography* 4 (4), 353–412.
- Samtleben, C., et al., 1995. Plankton in the Norwegian-Greenland Sea: from living communities to sediment assemblages—an actualistic approach. *Geologische Rundschau* 84 (1), 108–136.
- Scharek, R., et al., 1994. The transition from winter to early spring in the eastern Weddell Sea, Antarctica: plankton biomass and composition in relation to hydrography and nutrients. *Deep Sea Research Part I: Oceanographic Research Papers* 41 (8), 1231–1250.
- Schlitzer, R., 2008. *Ocean Data View*. <http://odv.awi.de>.
- Schmitz Jr., W.J., McCartney, M.S., 1993. On the North Atlantic circulation. *Rev. Geophys.* 31 (1), 29–49.
- Shackleton, N.J., Imbrie, J., Hall, M.A., 1983. Oxygen and carbon isotope record of East Pacific core V19-30: implications for the formation of deep water in the late Pleistocene North Atlantic. *Earth and Planetary Science Letters* 65 (2), 233–244.
- Shannon, C.E., Weaver, W., 1963. *The Mathematical Theory of Communication*. University of Illinois Press, 144 pp.
- Shimada, C., Sato, T., Toyoshima, S., Yamasaki, M., Tanimura, Y., 2008. Paleoeological significance of laminated diatomaceous oozes during the middle-to-late Pleistocene, North Atlantic Ocean (IODP Site U1304). *Marine Micropaleontology* 69 (2), 139–150.
- Stadum, C.J., Ling, H.-Y., 1969. Tripylean radiolaria in deep-sea sediments of the Norwegian Sea. *Micropaleontology* 15 (4), 481–489.
- Swanberg, N.R., Eide, L.K., 1992. The radiolarian fauna at the ice edge in the Greenland Sea during summer, 1988. *Journal of Marine Research* 50, 297–320.
- Swift, J.H., 1984. The circulation of the Denmark Strait and Iceland-Scotland overflow waters in the North Atlantic. *Deep Sea Research Part A. Oceanographic Research Papers* 31 (11), 1339–1355.
- Swift, J.H., Aagaard, K., 1981. Seasonal transitions and water mass formation in the Iceland and Greenland seas. *Deep Sea Research Part A. Oceanographic Research Papers* 28 (10), 1107–1129.
- Takahashi, K., 1991. Radiolaria: flux, ecology, and taxonomy in the Pacific and Atlantic. In: Honjo, S. (Ed.), *Ocean Biocenosis, Series No. 3*. Woods Hole Oceanographic Institution Press, pp. 1–303.
- Takahashi, K., 1994. From modern flux to paleoflux: assessment from sinking assemblages to thanatocoenosis. In: Zahn, R., Pedersen, T.F., Kaminski, M.A., Labeyrie, L. (Eds.), *Carbon Cycling in the Glacial Ocean: Constraints on the Ocean's Role in Global Change*. Springer-Verlag, Berlin, pp. 413–424.
- Takahashi, K., 1997. Time-series fluxes of Radiolaria in the eastern subarctic Pacific Ocean. *News of Osaka Micropaleontologists, Special Volume*, 10, pp. 299–309.
- Takahashi, K., Honjo, S., 1983. Radiolarian skeletons: size, weight, sinking speed, and residence time in tropical pelagic oceans. *Deep Sea Research Part A. Oceanographic Research Papers* 30 (5), 543–568.
- Takahashi, K., Hurd, D.C., Honjo, S., 1983. Phaeodarian skeletons: their role in silica transport to the deep sea. *Science* 222 (4624), 616–618.
- Takahashi, O., Mayama, S., Matsuoka, A., 2003. Host-symbiont associations of polycystine Radiolaria: epifluorescence microscopic observation of living Radiolaria. *Marine Micropaleontology* 49 (3), 187–194.
- Thomas, E., Booth, L., Maslin, M., Shackleton, N.J., 1995. Northeastern Atlantic benthic Foraminifera during the last 45,000 years: changes in productivity seen from the bottom up. *Paleoceanography* 10 (3), 545–562.
- Van Nieuwenhove, N., Bauch, H.A., Matthiessen, J., 2008. Last interglacial surface water conditions in the eastern Nordic Seas inferred from dinocyst and foraminiferal assemblages. *Marine Micropaleontology* 66 (3–4), 247–263.
- Venz, K.A., Hodell, D.A., Stanton, C., Warnke, D.A., 1999. A 1.0 Myr record of glacial North Atlantic intermediate water variability from ODP Site 982 in the Northeast Atlantic. *Paleoceanography* 14 (1), 42–52.
- Vidal, L., et al., 1997. Evidence for changes in the North Atlantic Deep Water linked to meltwater surges during the Heinrich events. *Earth and Planetary Science Letters* 146 (1–2), 13–27.
- Vidal, L., Labeyrie, L., van Weering, T.C.E., 1998. Benthic  $\delta^{18}\text{O}$  records in the North Atlantic over the last glacial period (60–10 kyr): evidence for brine formation. *Paleoceanography* 13 (3), 245–251.
- Wang, R., Abelman, A., 2002. Radiolarian responses to paleoceanographic events of the southern South China Sea during the Pleistocene. *Marine Micropaleontology* 46 (1–2), 25–44.
- Wang, R., Abelman, A., Li, B., Zhao, Q., 2000. Abrupt variations of the radiolarian fauna at Mid-Pleistocene climate transition in the South China Sea. *Chinese Science Bulletin* 45 (10), 952–955.
- Wright, A.K., Flower, B.P., 2002. Surface and deep ocean circulation in the subpolar North Atlantic during the mid-Pleistocene revolution. *Paleoceanography* 17 (4).
- Yamashita, H., Takahashi, K., Fujitani, N., 2002. Zonal and vertical distribution of radiolarians in the western and central Equatorial Pacific in January 1999. *Deep Sea Research Part II: Topical Studies in Oceanography* 49 (13–14), 2823–2862.